ARCHIVES OF CIVIL AND MECHANICAL ENGINEERING 18 (2018) 12–31

Available online at www.sciencedirect.com

ScienceDirect

journal homepage: http://www.elsevier.com/locate/acme

Original Research Article

Transient forced vibration response analysis of heterogeneous sandwich circular plates under viscoelastic boundary support

M.M. Alipour

Department of Mechanical Engineering, University of Mazandaran, Babolsar 47416-13534, Iran

ARTICLE INFO

Article history:
Received 8 January 2017
Accepted 24 May 2017
Available online 12 July 2017

Keywords:
Transient bending
Sandwich structures
Heterogeneous plate
Semi-analytical method
Viscoelastic boundary support

ABSTRACT

For the first time the transient bending analysis of a sandwich plate with viscoelastic boundary support is investigated in this study. Viscoelastic support consists of two sets of translational springs and dashpots connected in parallel along the in-plane and transverse directions. The sandwich plate is fabricated from heterogeneous face sheets where the material properties of each face sheets are assumed to be varied continuously in the radial direction according to a power-law function. Variations of the material properties of each face sheets are monitored by eight distinct inhomogeneity parameters. Therefore, the solution procedure may be used for a wide range of the practical problems. In order to investigate the effects of viscoelastic edge supports on the transient response of sandwich plate a wide range of the stiffness and damping coefficients of the edge supports in the in-plane and transverse directions are applied. Results of sandwich plates with the classical edge conditions as some special cases of the elastic/viscoelastic supports are compared with those extracted from the ABAQUS software based on the 3D theory of elasticity. The comparisons show that even for relatively complicated cases, there is a good agreement between the results.

1. Introduction

Sandwich plates are extensively used in many engineering fields. These structures are often subjected to dynamic loadings where control methods for elimination or reduction of the oscillations and the instabilities are very important in most applications. Viscoelastic boundary supports can be used as a control method to reduce the vibration of structures. On the other hands, plates are often connected to other members or supported by elastic or viscoelastic restraints, so the ideal classical boundary conditions (simply supported, clamped and free edges) cannot be applied for analysis of these structures. However, very few researches are carried out for dynamic analysis of these structures, even according to the ideal classical boundary conditions.

Some researchers analyzed the dynamic response of beam, single layer and sandwich plates under external applied loads. Among those, Shen et al. [1] studied the dynamic response of rectangular plates subjected to thermomechanical loading and resting on a Pasternak-type elastic foundation for simply supported boundary condition, based on the first-order shear

E-mail addresses: m.mollaalipour@umz.ac.ir, m.m.alipur@gmail.com.
http://dx.doi.org/10.1016/j.acme.2017.05.007

deformation theory. Civalek [2] carried out the static and dynamic analyses of thin rectangular plates resting on elastic foundation. Based on the first order shear deformation theory and using the finite element and shooting methods, Ribeiro investigated the forced vibrations of beams and plates [3] and laminated composite plates [4]. Pereira et al. [5] presented a dynamic formulation for the analysis of thick elastic plates, based on Reissner's theory and the boundary element method. Dynamic pull-in instability of vibrating nano-actuators is studied by Sedighi et al. [6]. Khalfi and Ross [7] investigated the transient and harmonic response of a sandwich with partial constrained layer damping. Based on the mesh-free method and three various theories such as the classical theory for analysis of thin plates, the first and third order shear deformations plate theories, transient analysis of homogeneous and FGM plates was performed by Sator et al. [8]. Wang and Shen [9] investigated the nonlinear dynamic response of sandwich plates with FGM face sheets resting on elastic foundations in thermal environments. Mojdehi et al. [10] carried out the three dimensional static and dynamic analysis of thick functionally graded plates based on the Meshless Local Petrov-Galerkin. Based on the zigzag-elasticity formulations, Alipour and Shariyat [11,12] investigated the dynamic stress and displacement response of functionally graded sandwich circular and annular plates. Kocatürk and Altintas [13] and Kocatürk et al. [14] investigated the steady-state response of viscoelastically point supported orthotropic rectangular plate based on the classical plate theory. Stembalski [15] used a friction damper for testing the vibration damping of a glass gatherer robot arm.

Also, modern structures are designed based on the use of inhomogeneous materials. Based on the higher-order shear deformation theory and using generalized differential quadrature method, Alinaghizadeh and Shariati performed the bending analysis of thick two-directional functionally graded annular sector and rectangular plates [16] and buckling analysis of thick radially functionally graded circular/annular sector plates [17] with variable thickness resting on elastic foundations. Based on the classical plate theory and using differential quadrature method, Hosseini-Hashemi et al. investigated free vibration [18] and buckling and free vibration [19] behaviors of radially functionally graded circular and annular sector thin plates resting on the Pasternak elastic foundation. Nosier and Fallah [20] analyzed the non-linear axisymmetric and asymmetric behavior of functionally graded circular plates under transverse mechanical loading based on the first-order shear deformation plate theory with von Karman non-linearity.

Structures may not always be analyzed based on the classical boundary conditions (ideal simply supported, clamped and free edges). However, very few researchers analyzed the plates with non-classical edge conditions where most of the existing studies were performed for static and free vibration analyses of elastically restrained structures based on the equivalent single layer theories. On the other hand, most of the existing researches were performed by using the classical plate theory [21–32]. The static and dynamic response of an elastically restrained rectangular plate, resting on a nonuniform elastic Winkler foundation were studied by Lee and Lin [21]. By using the Rayleigh–Ritz method, Nallim et al. [22] and Nallim and Grossi [23,24] performed the free vibration analysis of triangular symmetric composite plates, angle-ply symmetric laminated composite rectangular plates and symmetrically laminated elliptical and circular plates, respectively. Vescovini and Bisagni [25] studied the buckling and post-buckling behavior of composite panels. Free vibration of elastically restrained laminated composite plates were studied by Bahmyari and Rahbar-Ranji [26] and Ashour [27]. Bhaskara Rao and Kameswara Rao studied the buckling [28,29] analysis of circular plate and free vibration analysis of circular [30] and annular [31] plates. Post-buckling analysis of imperfect laminated composite plates was carried out by Chen and Qiao [32]. The influence of edge restraining stiffness on free vibration of thin homogeneous rectangular plate was examined by Jin et al. [33]. Some researchers employed the first order shear deformation theory for free vibration analysis of elastically supported plates [30–35]. Using the differential quadrature method, Malekzadeh at al. [34] and Sharma [35] analyzed the functionally graded annular and laminated sector plates, respectively. Dumir et al. [36] examined the large-amplitude axisymmetric free vibrations of cylindrically orthotropic thin circular plates of varying thicknesses. Gandhi et al. [37] studied the nonlinear axisymmetric static analysis of elastic orthotropic thin circular plates. Wang et al. [38] examined the functionally graded circular, annular and sector plates. Ye et al. [39] investigated the moderately thick composite laminated plates with internal line supports based on a modified Fourier solution procedure. Free in-plane vibration analysis of orthotropic rectangular plate with elastically restrained edges was performed by Zhang et al. [40] and Shi et al. [41]. Some researchers presented and applied theories for analysis of sandwich and multi-layered structures [42–46]. A novel economical analytical method was presented by Alipour [45] for bending and stress analysis of elastically restrained sandwich circular plates with functionally graded face sheets and core. Based on a novel solution procedure and layerwise method, also Alipour [46] examined the effects of elastically restrained edges on FG sandwich annular plates.

Very few researches may be found in literature on the analysis of sandwich plates with non-classical boundary conditions, even for static analysis of these structures. Based on the authors' knowledge, dynamic analyses of sandwich plates with viscoelastic boundary support have not been performed so far, even for the simple case of plates and using the equivalent single layer theories. In this study, the transient forced vibration response analysis of heterogeneous sandwich circular plates with viscoelastic boundary support are investigated for the first time. The viscoelastic support is simulated by using in-plane translational springs and dashpots connected in parallel along the in-plane and transverse directions. The material properties of each face sheets may be varied continuously in the radial direction according to a power-law function where variations of the material properties of each face sheets are monitored by eight distinct inhomogeneity parameters. Using the traditional equivalent single layer plate theories for analysis of the sandwich plates may lead to unreliable or erroneous results. Therefore, layerwise-zigzag theory is used for dynamic analysis of the sandwich plates. The governing equations of motion are derived based on the minimum total potential energy principle. A semi-analytical method which is a combination of the power series solution

[47–51] and the fourth-order Runge–Kutta [52] procedure is developed for solution of the extracted partial differential equations. To demonstrate the accuracy and efficiency of the presented analysis, the obtained results based on the proposed solution procedure for sandwich plates with the classical edge conditions as some special cases of the vicoelastic/elastic supports are compared with results of the three-dimensional theory of elasticity extracted from the ABAQUS software based on the finite element method. A wide range of the stiffness and damping coefficients of the edge supports in the in-plane and transverse directions are applied to investigate the effects of viscoelastic edge supports on the transient response of sandwich plate.

2. Governing equations of motion of the heterogeneous sandwich circular plates with viscoelastic boundary support

As shown in Fig. 1, a three-layer sandwich circular plate with radius b is considered. Thicknesses of the layers are denoted by h_1, h_2 and h_3.

Using the layerwise-zigzag theory [53,54] with the piece-wise linear local components, the displacement field of the layers may be written as:

$$\begin{aligned} &u_i(r,z_i) = u_0^{(i)}(r) + z_i\psi_r^{(i)}(r) \\ &w(r,z_i) = w(r) \quad -\frac{h_i}{2}\le z_i \le \frac{h_i}{2} \quad i=1,2,3 \end{aligned} \tag{1}$$

where $u_0^{(i)}$ and $\psi_r^{(i)}$ are the in-plane displacement of the point on the mid plane and the rotation of the radial section of each layer, w is the transverse deflection and z_1, z_2 and z_3 are three transverse local coordinates of each layer and measured from the mid-plane of the layers.

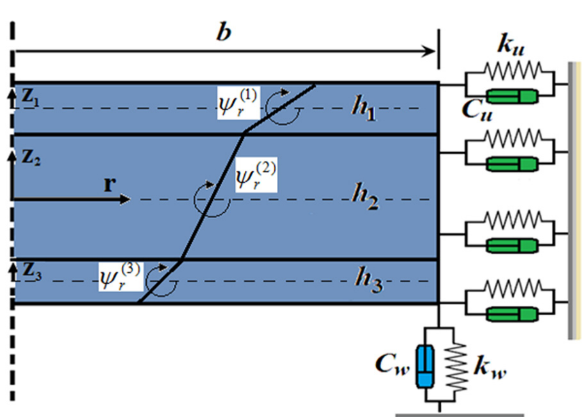

Fig. 1 – A schematic view of a sandwich circular plate with viscoelastic boundary support.

Based the continuity conditions of the displacement components at the interfaces between the layers $\left(u_1|_{z_1=-\frac{h_1}{2}} = u_2|_{z_2=\frac{h_2}{2}},\ u_2|_{z_2=-\frac{h_2}{2}} = u_3|_{z_3=\frac{h_3}{2}}\right)$, the in-plane displacement fields of the layers may be introduced as follows:

$$\begin{aligned} u_1 &= u_0 + \left(z_1 + \frac{h_1}{2}\right)\psi_r^{(1)} + \frac{h_2}{2}\psi_r^{(2)} \\ u_2 &= u_0 + z_2\psi_r^{(2)} \\ u_3 &= u_0 + \left(z_3 - \frac{h_3}{2}\right)\psi_r^{(3)} - \frac{h_2}{2}\psi_r^{(2)} \end{aligned} \tag{2}$$

where u_0 is the in-plane displacement of the point on the mid plane of the core.

In this section governing equations of motion of the heterogeneous sandwich circular plates with viscoelastic boundary support are derived based on the minimum total potential energy principle.

$$\delta\Pi = \delta U + \delta K - \delta W = 0, \tag{3}$$

where δU, δK and δW are increments of the strain energy, kinetic energy and work done by external loads, respectively.

$$\begin{aligned} \delta U &= \int_V (\sigma_r\delta\epsilon_r + \sigma_\theta\delta\epsilon_\theta + \tau_{rz}\delta\gamma_{rz})rd\theta drdz + \int_\Gamma [(K_w w + C_w\dot{w})\delta w]bd\theta|_{r=b} + \\ &\quad \int_h\int_\Gamma [(k_u u_1 + C_u u_1)\delta u_1 + (k_u u_2 + C_u\dot{u}_2)\delta u_2 + (k_u u_3 + C_u\dot{u}_3)\delta u_3]rd\theta dz|_{r=b} \\ \delta K &= \int_V \rho(\ddot{u}\delta u + \ddot{w}\delta w)dV \\ \delta W &= \int_A q\delta w dA \end{aligned} \tag{4}$$

where k_u and k_w (N/m^2) are the in-plane and transverse stiffness coefficients. C_u and C_w (N/m^2 s) are the in-plane and transverse damping coefficients. $\ddot{u}$ are $\ddot{w}$ are the acceleration parameters.

Based on Hooke's generalized stress–strain law and Cauchy's strain–displacement relation in the cylindrical coordinate system (r, θ, z), the linear stress-displacement relations may be written as:

$$\begin{aligned} \sigma_r^{(i)} &= \frac{E_i(r)}{1-\upsilon_i^2}\left(\epsilon_r^{(i)} + \upsilon_i\epsilon_\theta^{(i)}\right) = \frac{E_i(r)}{1-\upsilon_i^2}\left(u_{i,r} + \upsilon_i\frac{u_i}{r}\right) \\ \sigma_\theta^{(i)} &= \frac{E_i(r)}{1-\upsilon_i^2}\left(\epsilon_\theta^{(i)} + \upsilon_i\epsilon_r^{(i)}\right) = \frac{E_i(r)}{1-\upsilon_i^2}\left(\upsilon_i u_{i,r} + \frac{u_i}{r}\right) \\ \tau_{rz}^{(i)} &= \frac{E_i(r)}{2(1+\upsilon_i)}\gamma_{rz}^{(i)} = \frac{E_i(r)}{2(1+\upsilon_i)}(u_{i,z} + w_{,r}) \end{aligned} \tag{5}$$

where υ_i indicates the Poisson ratio of ith layer and the symbol "," stands for the partial derivative.

Different types of functions such as power-law [16,20] and exponential [17,19] functions can be used for material variation in heterogeneous plates.

For analysis of the sandwich plates with heterogeneous face sheets, variations of the elasticity modulus and the material density are described as follows:

$$\begin{aligned} E_1(r) &= \tilde{E}_1\left[1 + \alpha_1\left(\frac{r}{b}\right)^{\mu_1} + \beta_1\left(\frac{r}{b}\right)^{\eta_1}\right] \\ E_3(r) &= \tilde{E}_3\left[1 + \alpha_3\left(\frac{r}{b}\right)^{\mu_3} + \beta_3\left(\frac{r}{b}\right)^{\eta_3}\right] \\ \rho_1(r) &= \tilde{\rho}_1\left[1 + \gamma_1\left(\frac{r}{b}\right)^{\chi_1} + \lambda_1\left(\frac{r}{b}\right)^{\xi_1}\right] \\ \rho_3(r) &= \tilde{\rho}_3\left[1 + \gamma_3\left(\frac{r}{b}\right)^{\chi_3} + \lambda_3\left(\frac{r}{b}\right)^{\xi_3}\right] \end{aligned} \tag{6}$$

where α_j, μ_j, β_j, η_j, γ_j, χ_j, λ_j and ξ_j, $j = 1, 3$ are the inhomogeneity parameters of top ($j = 1$) and bottom face sheets ($j = 3$).

Substituting Eqs. (2), (4) and (5) into Eq. (3) and after some manipulations that are not included here for brevity, the governing equation of motion are extracted as five coupled partial governing equations.

$$\frac{N_r^{(1)}-N_\theta^{(1)}}{r}+N_{r,r}^{(1)}+\frac{N_r^{(2)}-N_\theta^{(2)}}{r}+N_{r,r}^{(2)}+\frac{N_r^{(3)}-N_\theta^{(3)}}{r}+N_{r,r}^{(3)}=\left(I_1^{(0)}+I_2^{(0)}+I_3^{(0)}\right)\ddot{u}_0+\frac{h_1}{2}I_1^{(0)}\ddot{\psi}_r^{(1)} +\frac{h_2}{2}\left(I_1^{(0)}-I_3^{(0)}\right)\ddot{\psi}_r^{(2)}-\frac{h_3}{2}I_3^{(0)}\ddot{\psi}_r^{(3)} \tag{7}$$

$$\frac{h_1}{2}\left(\frac{N_r^{(1)}-N_\theta^{(1)}}{r}+N_{r,r}^{(1)}\right)+\frac{M_r^{(1)}-M_\theta^{(1)}}{r}+M_{r,r}^{(1)}-Q_{rz}^{(1)}=\frac{h_1}{2}I_1^{(0)}\ddot{u}_0+\frac{h_1h_2}{4}I_1^{(0)}\ddot{\psi}_r^{(2)}+ \left(I_1^{(2)}+\frac{h_1^2}{4}I_1^{(0)}\right)\ddot{\psi}_r^{(1)} \tag{8}$$

$$\frac{h_2}{2}\left(\frac{N_r^{(1)}-N_\theta^{(1)}}{r}+N_{r,r}^{(1)}\right)-\frac{h_2}{2}\left(\frac{N_r^{(3)}-N_\theta^{(3)}}{r}+N_{r,r}^{(3)}\right)+\frac{M_r^{(2)}-M_\theta^{(2)}}{r}+M_{r,r}^{(2)}-Q_{rz}^{(2)}=\left(\frac{h_2}{2}I_1^{(0)}-\frac{h_2}{2}I_3^{(0)}\right)\ddot{u}_0 +\frac{h_1h_2}{4}I_1^{(0)}\ddot{\psi}_r^{(1)}+\left(\frac{h_2^2}{4}I_1^{(0)}+I_2^{(2)}+\frac{h_2^2}{4}I_3^{(0)}\right)\ddot{\psi}_r^{(2)}+\frac{h_2h_3}{4}I_3^{(0)}\ddot{\psi}_r^{(3)} \tag{9}$$

$$-\frac{h_3}{2}\left(\frac{N_r^{(3)}-N_\theta^{(3)}}{r}+N_{r,r}^{(3)}\right)+\frac{M_r^{(3)}-M_\theta^{(3)}}{r}+M_{r,r}^{(3)}-Q_{rz}^{(3)}=-\frac{h_3}{2}I_3^{(0)}\ddot{u}_0+\frac{h_2h_3}{4}I_3^{(0)}\ddot{\psi}_r^{(2)}+ \left(I_3^{(2)}+\frac{h_3^2}{4}I_3^{(0)}\right)\ddot{\psi}_r^{(3)} \tag{10}$$

$$Q_{r,r}^{(1)}+\frac{Q_r^{(1)}}{r}+Q_{r,r}^{(2)}+\frac{Q_r^{(2)}}{r}+Q_{r,r}^{(3)}+\frac{Q_r^{(3)}}{r}=q+(I_1^{(0)}+I_2^{(0)}+I_3^{(0)})\ddot{w} \tag{11}$$

where

$$\left\{\begin{matrix} N_i^{(k)} \\ M_i^{(k)} \end{matrix}\right\}=\int_{-\frac{h_k}{2}}^{\frac{h_k}{2}}\sigma_i^{(k)}\left\{\begin{matrix} 1 \\ z^{(k)} \end{matrix}\right\}dz^{(k)},\quad Q_r^{(k)}=\int_{-\frac{h_k}{2}}^{\frac{h_k}{2}}\tau_{rz}^{(k)}dz^{(k)},\quad k=1,2,3\quad i=r,\theta \tag{12}$$

$$\left\{\begin{matrix} I_1^{(0)} \\ I_1^{(2)} \end{matrix}\right\}=\int_{-\frac{h_1}{2}}^{\frac{h_1}{2}}\rho_1(r)\left\{\begin{matrix} 1 \\ z_1^2 \end{matrix}\right\}dz_1=\tilde{\rho}_1\left\{\begin{matrix} h_1 \\ \frac{h_1^3}{12} \end{matrix}\right\}\left[1+\gamma_1\left(\frac{r}{b}\right)^{\chi_1}+\lambda_1\left(\frac{r}{b}\right)^{\xi_1}\right]$$
$$\left\{\begin{matrix} I_2^{(0)} \\ I_2^{(2)} \end{matrix}\right\}=\int_{-\frac{h_1}{2}}^{\frac{h_1}{2}}\rho_2(r)\left\{\begin{matrix} 1 \\ z_2^2 \end{matrix}\right\}dz_2=\rho_2\left\{\begin{matrix} h_2 \\ \frac{h_2^3}{12} \end{matrix}\right\} \tag{13}$$
$$\left\{\begin{matrix} I_3^{(0)} \\ I_3^{(2)} \end{matrix}\right\}=\int_{-\frac{h_3}{2}}^{\frac{h_3}{2}}\rho_3(r)\left\{\begin{matrix} 1 \\ z_3^2 \end{matrix}\right\}dz_3=\tilde{\rho}_3\left\{\begin{matrix} h_3 \\ \frac{h_3^3}{12} \end{matrix}\right\}\left[1+\gamma_3\left(\frac{r}{b}\right)^{\chi_3}+\lambda_3\left(\frac{r}{b}\right)^{\xi_3}\right]$$

Based on Eqs. (2) and (5), Eqs. (12) may be rewritten in the following form:

$$\left\{\begin{matrix} N_r^{(1)} \\ N_\theta^{(1)} \end{matrix}\right\}=\frac{\tilde{E}_1h_1}{1-\upsilon_1^2}\left[\left\{\begin{matrix} 1 \\ \upsilon_1 \end{matrix}\right\}\left(u_{0,r}+\frac{h_1}{2}\psi_{r,r}^{(1)}+\frac{h_2}{2}\psi_{r,r}^{(2)}\right)+\left\{\begin{matrix} \upsilon_1 \\ 1 \end{matrix}\right\}\frac{1}{r}\left(u_0+\frac{h_1}{2}\psi_r^{(1)}+\frac{h_2}{2}\psi_r^{(2)}\right)\right]\left[1+\alpha_1\left(\frac{r}{b}\right)^{\mu_1}+\beta_1\left(\frac{r}{b}\right)^{\eta_1}\right],$$
$$\left\{\begin{matrix} N_r^{(2)} \\ N_\theta^{(2)} \end{matrix}\right\}=\frac{E_2h_2}{1-\upsilon_2^2}\left[\left\{\begin{matrix} 1 \\ \upsilon_2 \end{matrix}\right\}u_{0,r}+\left\{\begin{matrix} \upsilon_2 \\ 1 \end{matrix}\right\}\frac{u_0}{r}\right], \tag{14}$$
$$\left\{\begin{matrix} N_r^{(3)} \\ N_\theta^{(3)} \end{matrix}\right\}=\frac{\tilde{E}_3h_3}{1-\upsilon_3^2}\left[\left\{\begin{matrix} 1 \\ \upsilon_3 \end{matrix}\right\}\left(u_{0,r}-\frac{h_3}{2}\psi_{r,r}^{(3)}-\frac{h_2}{2}\psi_{r,r}^{(2)}\right)+\left\{\begin{matrix} \upsilon_3 \\ 1 \end{matrix}\right\}\frac{1}{r}\left(u_0-\frac{h_3}{2}\psi_r^{(3)}-\frac{h_2}{2}\psi_r^{(2)}\right)\right]\left[1+\alpha_3\left(\frac{r}{b}\right)^{\mu_3}+\beta_3\left(\frac{r}{b}\right)^{\eta_3}\right]$$

$$\left\{\begin{matrix} M_r^{(1)} \\ M_\theta^{(1)} \end{matrix}\right\}=\frac{\tilde{E}_1h_1^3}{12(1-\upsilon_1^2)}\left(\left\{\begin{matrix} 1 \\ \upsilon_1 \end{matrix}\right\}\psi_{r,r}^{(1)}+\left\{\begin{matrix} \upsilon_1 \\ 1 \end{matrix}\right\}\frac{1}{r}\psi_r^{(1)}\right)\left[1+\alpha_1\left(\frac{r}{b}\right)^{\mu_1}+\beta_1\left(\frac{r}{b}\right)^{\eta_1}\right],$$
$$\left\{\begin{matrix} M_r^{(2)} \\ M_\theta^{(2)} \end{matrix}\right\}=\frac{E_2h_2^3}{12(1-\upsilon_2^2)}\left(\left\{\begin{matrix} 1 \\ \upsilon_2 \end{matrix}\right\}\psi_{r,r}^{(2)}+\left\{\begin{matrix} \upsilon_2 \\ 1 \end{matrix}\right\}\frac{1}{r}\psi_r^{(2)}\right) \tag{15}$$
$$\left\{\begin{matrix} M_r^{(3)} \\ M_\theta^{(3)} \end{matrix}\right\}=\frac{\tilde{E}_3h_3^3}{12(1-\upsilon_3^2)}\left(\left\{\begin{matrix} 1 \\ \upsilon_3 \end{matrix}\right\}\psi_{r,r}^{(3)}+\left\{\begin{matrix} \upsilon_3 \\ 1 \end{matrix}\right\}\frac{1}{r}\psi_r^{(3)}\right)\left[1+\alpha_3\left(\frac{r}{b}\right)^{\mu_3}+\beta_3\left(\frac{r}{b}\right)^{\eta_3}\right]$$

$$\begin{cases} Q_r^{(1)} = \dfrac{\tilde{E}_1 h_1}{2(1+\upsilon_1)}\left(\psi_r^{(1)} + w_{,r}\right)\left[1+\alpha_1\left(\dfrac{r}{b}\right)^{\mu_1} + \beta_1\left(\dfrac{r}{b}\right)^{\eta_1}\right], \\ Q_r^{(2)} = \dfrac{E_2 h_2}{2(1+\upsilon_2)}\left(\psi_r^{(2)} + w_{,r}\right) \\ Q_r^{(3)} = \dfrac{\tilde{E}_3 h_3}{2(1+\upsilon_3)}\left(\psi_r^{(3)} + w_{,r}\right)\left[1+\alpha_3\left(\dfrac{r}{b}\right)^{\mu_3} + \beta_3\left(\dfrac{r}{b}\right)^{\eta_3}\right] \end{cases} \tag{16}$$

Based on Eqs. (13)–(16), the governing equations (7)–(11) may be rewritten as:

$$\begin{aligned} &\left\{\frac{\tilde{E}_1 h_1}{1-\upsilon_1^2}\left[1+\alpha_1\left(\frac{r}{b}\right)^{\mu_1}+\beta_1\left(\frac{r}{b}\right)^{\eta_1}\right]+\frac{E_2 h_2}{1-\upsilon_2^2}+\frac{\tilde{E}_3 h_3}{1-\upsilon_3^2}\left[1+\alpha_3\left(\frac{r}{b}\right)^{\mu_3}+\beta_3\left(\frac{r}{b}\right)^{\eta_3}\right]\right\}\left(u_{0,rr}+\frac{u_{0,r}}{r}-\frac{u_0}{r^2}\right) \\ &+\frac{\tilde{E}_1 h_1^2}{2(1-\upsilon_1^2)}\left[1+\alpha_1\left(\frac{r}{b}\right)^{\mu_1}+\beta_1\left(\frac{r}{b}\right)^{\eta_1}\right]\left(\psi_{r,rr}^{(1)}+\frac{\psi_{r,r}^{(1)}}{r}-\frac{\psi_r^{(1)}}{r^2}\right)-\frac{\tilde{E}_3 h_3^2}{2(1-\upsilon_3^2)}\left[1+\alpha_3\left(\frac{r}{b}\right)^{\mu_3}+\beta_3\left(\frac{r}{b}\right)^{\eta_3}\right]\left(\psi_{r,rr}^{(3)}+\frac{\psi_{r,r}^{(3)}}{r}-\frac{\psi_r^{(3)}}{r^2}\right) \\ &+\frac{h_2}{2}\left\{\frac{\tilde{E}_1 h_1}{1-\upsilon_1^2}\left[1+\alpha_1\left(\frac{r}{b}\right)^{\mu_1}+\beta_1\left(\frac{r}{b}\right)^{\eta_1}\right]-\frac{\tilde{E}_3 h_3}{1-\upsilon_3^2}\left[1+\alpha_3\left(\frac{r}{b}\right)^{\mu_3}+\beta_3\left(\frac{r}{b}\right)^{\eta_3}\right]\right\}\left(\psi_{r,rr}^{(2)}+\frac{\psi_{r,r}^{(2)}}{r}-\frac{\psi_r^{(2)}}{r^2}\right) \\ &+\frac{1}{b}\frac{\tilde{E}_1 h_1}{1-\upsilon_1^2}\left[\alpha_1\mu_1\left(\frac{r}{b}\right)^{\mu_1-1}+\beta_1\eta_1\left(\frac{r}{b}\right)^{\eta_1-1}\right]\left[\left(u_{0,r}+\frac{h_1}{2}\psi_{r,r}^{(1)}+\frac{h_2}{2}\psi_{r,r}^{(2)}\right)+\frac{\upsilon_1}{r}\left(u_0+\frac{h_1}{2}\psi_r^{(1)}+\frac{h_2}{2}\psi_r^{(2)}\right)\right] \\ &+\frac{1}{b}\frac{\tilde{E}_3 h_3}{1-\upsilon_3^2}\left[\alpha_3\mu_3\left(\frac{r}{b}\right)^{\mu_3-1}+\beta_3\eta_3\left(\frac{r}{b}\right)^{\eta_3-1}\right]\left[\left(u_{0,r}-\frac{h_3}{2}\psi_{r,r}^{(3)}-\frac{h_2}{2}\psi_{r,r}^{(2)}\right)+\frac{\upsilon_3}{r}\left(u_0-\frac{h_3}{2}\psi_r^{(3)}-\frac{h_2}{2}\psi_r^{(2)}\right)\right] \\ &=\tilde{\rho}_1 h_1\left[1+\gamma_1\left(\frac{r}{b}\right)^{\chi_1}+\lambda_1\left(\frac{r}{b}\right)^{\xi_1}\right]\ddot{u}_0+\rho_2 h_2\ddot{u}_0+\tilde{\rho}_3 h_3\left[1+\gamma_3\left(\frac{r}{b}\right)^{\chi_3}+\lambda_3\left(\frac{r}{b}\right)^{\xi_3}\right]\ddot{u}_0 \\ &+\frac{h_1^2}{2}\tilde{\rho}_1\left[1+\gamma_1\left(\frac{r}{b}\right)^{\chi_1}+\lambda_1\left(\frac{r}{b}\right)^{\xi_1}\right]\ddot{\psi}_r^{(1)}-\frac{h_3^2}{2}\tilde{\rho}_3\left[1+\gamma_3\left(\frac{r}{b}\right)^{\chi_3}+\lambda_3\left(\frac{r}{b}\right)^{\xi_3}\right]\ddot{\psi}_r^{(3)} \\ &+\frac{h_2}{2}\left\{\tilde{\rho}_1 h_1\left[1+\gamma_1\left(\frac{r}{b}\right)^{\chi_1}+\lambda_1\left(\frac{r}{b}\right)^{\xi_1}\right]-\tilde{\rho}_3 h_3\left[1+\gamma_3\left(\frac{r}{b}\right)^{\chi_3}+\lambda_3\left(\frac{r}{b}\right)^{\xi_3}\right]\right\}\ddot{\psi}_r^{(2)} \end{aligned} \tag{17}$$

$$\begin{aligned} &\frac{h_1}{2}\frac{\tilde{E}_1 h_1}{1-\upsilon_1^2}\left[1+\alpha_1\left(\frac{r}{b}\right)^{\mu_1}+\beta_1\left(\frac{r}{b}\right)^{\eta_1}\right]\left(u_{0,rr}+\frac{u_{0,r}}{r}-\frac{u_0}{r^2}\right)+ \\ &\left(\frac{h_1^2}{4}\frac{\tilde{E}_1 h_1}{1-\upsilon_1^2}+\frac{\tilde{E}_1 h_1^3}{12(1-\upsilon_1^2)}\right)\left[1+\alpha_1\left(\frac{r}{b}\right)^{\mu_1}+\beta_1\left(\frac{r}{b}\right)^{\eta_1}\right]\left(\psi_{r,rr}^{(1)}+\frac{\psi_{r,r}^{(1)}}{r}-\frac{\psi_r^{(1)}}{r^2}\right)+ \\ &\frac{\tilde{E}_1 h_1}{1-\upsilon_1^2}\left[1+\alpha_1\left(\frac{r}{b}\right)^{\mu_1}+\beta_1\left(\frac{r}{b}\right)^{\eta_1}\right]\left[\frac{h_1 h_2}{4}\left(\psi_{r,rr}^{(2)}+\frac{\psi_{r,r}^{(2)}}{r}-\frac{\psi_r^{(2)}}{r^2}\right)-\frac{1-\upsilon_1}{2}\left(\psi_r^{(1)}+w_{,r}\right)\right]+ \\ &\frac{h_1}{2}\frac{\tilde{E}_1 h_1}{1-\upsilon_1^2}\left[\left(u_{0,r}+\frac{h_1}{2}\psi_{r,r}^{(1)}+\frac{h_2}{2}\psi_{r,r}^{(2)}\right)+\frac{\upsilon_1}{r}\left(u_0+\frac{h_1}{2}\psi_r^{(1)}+\frac{h_2}{2}\psi_r^{(2)}\right)\right]\left[\frac{\mu_1}{b}\alpha_1\left(\frac{r}{b}\right)^{\mu_1-1}+\frac{\eta_1}{b}\beta_1\left(\frac{r}{b}\right)^{\eta_1-1}\right]+ \\ &\frac{\tilde{E}_1 h_1^3}{12(1-\upsilon_1^2)}\left(\psi_{r,r}^{(1)}+\frac{\upsilon_1}{r}\psi_r^{(1)}\right)\left[\frac{\mu_1}{b}\alpha_1\left(\frac{r}{b}\right)^{\mu_1-1}+\frac{\eta_1}{b}\beta_1\left(\frac{r}{b}\right)^{\eta_1-1}\right] \\ &=\left[1+\gamma_1\left(\frac{r}{b}\right)^{\chi_1}+\lambda_1\left(\frac{r}{b}\right)^{\xi_1}\right]\left[\frac{h_1}{2}\tilde{\rho}_1 h_1\left(\ddot{u}_0+\frac{h_2}{2}\ddot{\psi}_r^{(2)}+\frac{h_1}{2}\ddot{\psi}_r^{(1)}\right)+\tilde{\rho}_1\frac{h_1^3}{12}\ddot{\psi}_r^{(1)}\right] \end{aligned} \tag{18}$$

$$\begin{aligned} &\frac{h_2}{2}\left\{\frac{\tilde{E}_1 h_1}{1-\upsilon_1^2}\left[1+\alpha_1\left(\frac{r}{b}\right)^{\mu_1}+\beta_1\left(\frac{r}{b}\right)^{\eta_1}\right]-\frac{\tilde{E}_3 h_3}{1-\upsilon_3^2}\left[1+\alpha_3\left(\frac{r}{b}\right)^{\mu_3}+\beta_3\left(\frac{r}{b}\right)^{\eta_3}\right]\right\}\left(u_{0,rr}+\frac{u_{0,r}}{r}-\frac{u_0}{r^2}\right) \\ &+\frac{h_1 h_2}{4}\frac{\tilde{E}_1 h_1}{1-\upsilon_1^2}\left[1+\alpha_1\left(\frac{r}{b}\right)^{\mu_1}+\beta_1\left(\frac{r}{b}\right)^{\eta_1}\right]\left(\psi_{r,rr}^{(1)}+\frac{\psi_{r,r}^{(1)}}{r}-\frac{\psi_r^{(1)}}{r^2}\right) \\ &+\left\{\frac{h_2^2}{4}\frac{\tilde{E}_1 h_1}{1-\upsilon_1^2}\left[1+\alpha_1\left(\frac{r}{b}\right)^{\mu_1}+\beta_1\left(\frac{r}{b}\right)^{\eta_1}\right]+\frac{E_2 h_2^3}{12(1-\upsilon_2^2)}+\frac{h_2^2}{4}\frac{\tilde{E}_3 h_3}{1-\upsilon_3^2}\left[1+\alpha_3\left(\frac{r}{b}\right)^{\mu_3}+\beta_3\left(\frac{r}{b}\right)^{\eta_3}\right]\right\}\left(\psi_{r,rr}^{(2)}+\frac{\psi_{r,r}^{(2)}}{r}-\frac{\psi_r^{(2)}}{r^2}\right) \\ &+\frac{h_2 h_3}{4}\frac{\tilde{E}_3 h_3}{1-\upsilon_3^2}\left[1+\alpha_3\left(\frac{r}{b}\right)^{\mu_3}+\beta_3\left(\frac{r}{b}\right)^{\eta_3}\right]\left(\psi_{r,rr}^{(3)}+\frac{\psi_{r,r}^{(3)}}{r}-\frac{\psi_r^{(3)}}{r^2}\right)-\frac{E_2 h_2}{2(1+\upsilon_2)}\left(\psi_r^{(2)}+w_{,r}\right) \\ &+\frac{h_2}{2}\frac{\tilde{E}_1 h_1}{1-\upsilon_1^2}\left[\left(u_{0,r}+\frac{h_1}{2}\psi_{r,r}^{(1)}+\frac{h_2}{2}\psi_{r,r}^{(2)}\right)+\frac{\upsilon_1}{r}\left(u_0+\frac{h_1}{2}\psi_r^{(1)}+\frac{h_2}{2}\psi_r^{(2)}\right)\right]\left[\frac{\mu_1}{b}\alpha_1\left(\frac{r}{b}\right)^{\mu_1-1}+\frac{\eta_1}{b}\beta_1\left(\frac{r}{b}\right)^{\eta_1-1}\right], \\ &-\frac{h_2}{2}\frac{\tilde{E}_3 h_3}{1-\upsilon_3^2}\left[\left(u_{0,r}-\frac{h_3}{2}\psi_{r,r}^{(3)}-\frac{h_2}{2}\psi_{r,r}^{(2)}\right)+\frac{\upsilon_3}{r}\left(u_0-\frac{h_3}{2}\psi_r^{(3)}-\frac{h_2}{2}\psi_r^{(2)}\right)\right]\left[\frac{\mu_3}{b}\alpha_3\left(\frac{r}{b}\right)^{\mu_3-1}+\frac{\eta_3}{b}\beta_3\left(\frac{r}{b}\right)^{\eta_3-1}\right] \\ &=\frac{h_2}{2}\tilde{\rho}_1 h_1\left[1+\gamma_1\left(\frac{r}{b}\right)^{\chi_1}+\lambda_1\left(\frac{r}{b}\right)^{\xi_1}\right]\left(\ddot{u}_0+\frac{h_1}{2}\ddot{\psi}_r^{(1)}+\frac{h_2}{2}\ddot{\psi}_r^{(2)}\right)+\rho_2\frac{h_2^3}{12}\ddot{\psi}_r^{(2)}+ \\ &\frac{h_2}{2}\tilde{\rho}_3 h_3\left[1+\gamma_3\left(\frac{r}{b}\right)^{\chi_3}+\lambda_3\left(\frac{r}{b}\right)^{\xi_3}\right]\left(-\ddot{u}_0+\frac{h_2}{2}\ddot{\psi}_r^{(2)}+\frac{h_3}{2}\ddot{\psi}_r^{(3)}\right) \end{aligned} \tag{19}$$

$$
\begin{aligned}
&-\frac{h_3}{2}\frac{\tilde{E}_3 h_3}{1-\upsilon_3^2}\left[1+\alpha_3\left(\frac{r}{b}\right)^{\mu_3}+\beta_3\left(\frac{r}{b}\right)^{\eta_3}\right]\left(u_{0,rr}+\frac{u_{0,r}}{r}-\frac{u_0}{r^2}\right)\\
&+\frac{h_2 h_3}{4}\frac{\tilde{E}_3 h_3}{1-\upsilon_3^2}\left[1+\alpha_3\left(\frac{r}{b}\right)^{\mu_3}+\beta_3\left(\frac{r}{b}\right)^{\eta_3}\right]\left(\psi_{r,rr}^{(2)}+\frac{\psi_{r,r}^{(2)}}{r}-\frac{\psi_r^{(2)}}{r^2}\right)\\
&+\left[1+\alpha_3\left(\frac{r}{b}\right)^{\mu_3}+\beta_3\left(\frac{r}{b}\right)^{\eta_3}\right]\left[\left(\frac{\tilde{E}_3 h_3^3}{12(1-\upsilon_3^2)}+\frac{h_3^2}{4}\frac{\tilde{E}_3 h_3}{1-\upsilon_3^2}\right)\left(\psi_{r,rr}^{(3)}+\frac{\psi_{r,r}^{(3)}}{r}-\frac{\psi_r^{(3)}}{r^2}\right)-\frac{1-\upsilon_3}{2}\frac{\tilde{E}_3 h_3}{1-\upsilon_3^2}\left(\psi_r^{(3)}+w_{,r}\right)\right]\\
&-\frac{h_3}{2}\frac{\tilde{E}_3 h_3}{1-\upsilon_3^2}\left[\left(u_{0,r}-\frac{h_3}{2}\psi_{r,r}^{(3)}-\frac{h_2}{2}\psi_{r,r}^{(2)}\right)+\frac{\upsilon_3}{r}\left(u_0-\frac{h_3}{2}\psi_r^{(3)}-\frac{h_2}{2}\psi_r^{(2)}\right)\right]\left[\frac{\mu_3}{b}\alpha_3\left(\frac{r}{b}\right)^{\mu_3-1}+\frac{\eta_3}{b}\beta_3\left(\frac{r}{b}\right)^{\eta_3-1}\right]\\
&+\frac{\tilde{E}_3 h_3^3}{12(1-\upsilon_3^2)}\left(\psi_{r,r}^{(3)}+\frac{\upsilon_3}{r}\psi_r^{(3)}\right)\left[\frac{\mu_3}{b}\alpha_3\left(\frac{r}{b}\right)^{\mu_3-1}+\frac{\eta_3}{b}\beta_3\left(\frac{r}{b}\right)^{\eta_3-1}\right]\\
&=\left[1+\gamma_3\left(\frac{r}{b}\right)^{\chi_3}+\lambda_3\left(\frac{r}{b}\right)^{\xi_3}\right]\left[\frac{h_3}{2}\tilde{\rho}_3 h_3\left(-\ddot{u}_0+\frac{h_2}{2}\ddot{\psi}_r^{(2)}+\frac{h_3}{2}\ddot{\psi}_r^{(3)}\right)+\tilde{\rho}_3\frac{h_3^3}{12}\ddot{\psi}_r^{(3)}\right]
\end{aligned}
\tag{20}
$$

$$
\begin{aligned}
&\left\{\frac{\tilde{E}_1 h_1}{2(1+\upsilon_1)}\left[1+\alpha_1\left(\frac{r}{b}\right)^{\mu_1}+\beta_1\left(\frac{r}{b}\right)^{\eta_1}\right]+\frac{E_2 h_2}{2(1+\upsilon_2)}+\frac{\tilde{E}_3 h_3}{2(1+\upsilon_3)}\left[1+\alpha_3\left(\frac{r}{b}\right)^{\mu_3}+\beta_3\left(\frac{r}{b}\right)^{\eta_3}\right]\right\}\left(w_{,rr}+\frac{w_{,r}}{r}\right)\\
&+\frac{\tilde{E}_1 h_1}{2(1+\upsilon_1)}\left[1+\alpha_1\left(\frac{r}{b}\right)^{\mu_1}+\beta_1\left(\frac{r}{b}\right)^{\eta_1}\right]\left(\psi_{r,r}^{(1)}+\frac{\psi_r^{(1)}}{r}\right)+\frac{E_2 h_2}{2(1+\upsilon_2)}\left(\psi_{r,r}^{(2)}+\frac{\psi_r^{(2)}}{r}\right)\\
&+\frac{\tilde{E}_3 h_3}{2(1+\upsilon_3)}\left[1+\alpha_3\left(\frac{r}{b}\right)^{\mu_3}+\beta_3\left(\frac{r}{b}\right)^{\eta_3}\right]\left(\psi_{r,r}^{(3)}+\frac{\psi_r^{(3)}}{r}\right)+\frac{\tilde{E}_1 h_1}{2(1+\upsilon_1)}\left[\frac{\mu_1}{b}\alpha_1\left(\frac{r}{b}\right)^{\mu_1-1}+\frac{\eta_1}{b}\beta_1\left(\frac{r}{b}\right)^{\eta_1-1}\right]\left(\psi_r^{(1)}+w_{,r}\right)\\
&+\frac{\tilde{E}_3 h_3}{2(1+\upsilon_3)}\left[\frac{\mu_3}{b}\alpha_3\left(\frac{r}{b}\right)^{\mu_3-1}+\frac{\eta_3}{b}\beta_3\left(\frac{r}{b}\right)^{\eta_3-1}\right]\left(\psi_r^{(3)}+w_{,r}\right)\\
&=-q+\left\{\tilde{\rho}_1 h_1\left[1+\gamma_1\left(\frac{r}{b}\right)^{\chi_1}+\lambda_1\left(\frac{r}{b}\right)^{\xi_1}\right]+\rho_2 h_2+\tilde{\rho}_3 h_3\left[1+\gamma_3\left(\frac{r}{b}\right)^{\chi_3}+\lambda_3\left(\frac{r}{b}\right)^{\xi_3}\right]\right\}\ddot{w}
\end{aligned}
\tag{21}
$$

The governing equations of axisymmetric circular plates (17)–(21) have to be solved along with the boundary conditions, the regularity conditions at the center of the plate and the initial conditions.

For sandwich plates with viscoelastic boundary support as shown in Fig. 1, the general boundary conditions can be described as follows:

$$
\begin{aligned}
&\left[N_r^{(1)}+N_r^{(2)}+N_r^{(3)}+(h_1+h_2+h_3)(k_u u_0+C_u\dot{u}_0)+\frac{h_1^2}{2}\left(k_u\psi_r^{(1)}+C_u\dot{\psi}_r^{(1)}\right)+\right.\\
&\qquad\left.\left.\frac{h_2}{2}(h_1-h_3)\left(k_u\psi_r^{(2)}+C_u\dot{\psi}_r^{(2)}\right)-\frac{h_3^2}{2}\left(k_u\psi_r^{(3)}+C_u\dot{\psi}_r^{(3)}\right)\right]\right|_{r=b}=0
\end{aligned}
\tag{22}
$$

$$
\begin{aligned}
&\left[\frac{h_1}{2}N_r^{(1)}+M_r^{(1)}+\frac{h_1^3}{12}\left(k_u\psi_r^{(1)}+C_u\dot{\psi}_r^{(1)}\right)+\frac{h_1^2}{2}k_u\left(u_0+\frac{h_1}{2}\psi_r^{(1)}+\frac{h_2}{2}\psi_r^{(2)}\right)+\right.\\
&\qquad\left.\left.\frac{h_1^2}{2}C_u\left(\dot{u}_0+\frac{h_1}{2}\dot{\psi}_r^{(1)}+\frac{h_2}{2}\dot{\psi}_r^{(2)}\right)\right]\right|_{r=b}=0
\end{aligned}
\tag{23}
$$

$$
\begin{aligned}
&\left[\frac{h_2}{2}\left(N_r^{(1)}-N_r^{(3)}\right)+M_r^{(2)}+\frac{h_2}{2}(h_1-h_3)(k_u u_0+C_u\dot{u}_0)+\frac{h_2}{2}\frac{h_1^2}{2}\left(k_u\psi_r^{(1)}+C_u\dot{\psi}_r^{(1)}\right)+\right.\\
&\qquad\left.\left.\frac{h_2^2}{4}\left(h_1+\frac{h_2}{3}+h_3\right)\left(k_u\psi_r^{(2)}+C_u\dot{\psi}_r^{(2)}\right)+\frac{h_2}{2}\frac{h_3^2}{2}\left(k_u\psi_r^{(3)}+C_u\dot{\psi}_r^{(3)}\right)\right]\right|_{r=b}=0
\end{aligned}
\tag{24}
$$

$$
\begin{aligned}
&\left[-\frac{h_3}{2}N_r^{(3)}+M_r^{(3)}+\frac{h_3^3}{12}\left(k_u\psi_r^{(3)}+C_u\dot{\psi}_r^{(3)}\right)-\frac{h_3^2}{2}k_u\left(u_0-\frac{h_3}{2}\psi_r^{(3)}-\frac{h_2}{2}\psi_r^{(2)}\right)\right.\\
&\qquad\left.\left.-\frac{h_3^2}{2}C_u\left(\dot{u}_0-\frac{h_3}{2}\dot{\psi}_r^{(3)}-\frac{h_2}{2}\dot{\psi}_r^{(2)}\right)\right]\right|_{r=b}=0
\end{aligned}
\tag{25}
$$

$$
\left.\left(Q_r^{(1)}+Q_r^{(2)}+Q_r^{(3)}+k_w w+C_w\dot{w}\right)\right|_{r=b}=0 \tag{26}
$$

The regularity conditions:

$$\begin{aligned}
&u(0,t)=0,\\
&\psi_r^{(1)}(0,t)=0,\\
&\psi_r^{(2)}(0,t)=0,\\
&\psi_r^{(3)}(0,t)=0,\\
&w_{,r}(0,t)=0.
\end{aligned} \tag{27}$$

the initial conditions:

$$\begin{aligned}
&u(r,0)=\dot{u}(r,0)=0,\\
&\psi_r^{(1)}(r,0)=\dot{\psi}_r^{(1)}(r,0)=0,\\
&\psi_r^{(2)}(r,0)=\dot{\psi}_r^{(2)}(r,0)=0,\\
&\psi_r^{(3)}(r,0)=\dot{\psi}_r^{(3)}(r,0)=0,\\
&w(r,0)=\dot{w}(r,0)=0.
\end{aligned} \tag{28}$$

$\dot{u}, \dot{\psi}_r^{(1)}, \dot{\psi}_r^{(2)}, \dot{\psi}_r^{(3)}$ and $\dot{w}$ are the velocity parameters.

3. Solution of the extracted partial differential equations

On the basis of the power series solution in the space domain and the fourth-order Runge–Kutta procedure in the time domain, the semi-analytical solution is developed for solution of the coupled partial differential equations.

To present a more general solution, the following non-dimensional parameters are introduced:

$$\overline{u}_0=\frac{u_0}{b},\quad \overline{w}=\frac{w}{b},\quad R=\frac{r}{b},\quad \tau_1=\frac{h_1}{b},\quad \tau_2=\frac{h_2}{b},\quad \tau_3=\frac{h_3}{b}, \tag{29}$$

The unknown displacement, velocity and acceleration functions are analytic in the R domain and can be represented in terms of power series.

$$\begin{aligned}
&\overline{u}_0(R,t=j\Delta t)=\sum_{i=0}^{\infty}U_{i,j}R^i,\quad \psi_r^{(1)}(R,t=j\Delta t)=\sum_{x=0}^{\infty}X_{i,j}^{(1)}R^i,\quad \psi_r^{(2)}(R,t=j\Delta t)=\sum_{x=0}^{\infty}X_{i,j}^{(2)}R^i,\\
&\psi_r^{(3)}(R,t=j\Delta t)=\sum_{x=0}^{\infty}X_{i,j}^{(3)}R^i,\quad \overline{w}(R,t=j\Delta t)=\sum_{x=0}^{\infty}W_{i,j}R^i
\end{aligned} \tag{30}$$

$$\begin{aligned}
&\dot{\overline{u}}_0(R,t=j\ \Delta t)=\sum_{i=0}^{\infty}\dot{U}_{i,j}R^i,\quad \dot{\psi}_r^{(1)}(R,t=j\ \Delta t)=\sum_{x=0}^{\infty}\dot{X}_{i,j}^{(1)}R^i,\quad \dot{\psi}_r^{(2)}(R,t=j\,\Delta t)=\sum_{x=0}^{\infty}\dot{X}_{i,j}^{(2)}R^i,\\
&\dot{\psi}_r^{(3)}(R,t=j\,\Delta t)=\sum_{x=0}^{\infty}\dot{X}_{i,j}^{(3)}R^i,\quad \dot{\overline{w}}(R,t=j\,\Delta t)=\sum_{x=0}^{\infty}\dot{W}_{i,j}R^i
\end{aligned} \tag{31}$$

$$\begin{aligned}
&\ddot{\overline{u}}_0(R,t=j\Delta t)=\sum_{i=0}^{\infty}\ddot{U}_{i,j}R^i,\quad \ddot{\psi}_r^{(1)}(R,t=j\Delta t)=\sum_{x=0}^{\infty}\ddot{X}_{i,j}^{(1)}R^i,\quad \ddot{\psi}_r^{(2)}(R,t=j\Delta t)=\sum_{x=0}^{\infty}\ddot{X}_{i,j}^{(2)}R^i,\\
&\ddot{\psi}_r^{(3)}(R,t=j\Delta t)=\sum_{x=0}^{\infty}\ddot{X}_{i,j}^{(3)}R^i,\quad \ddot{\overline{w}}(R,t=j\Delta t)=\sum_{x=0}^{\infty}\ddot{W}_{i,j}R^i
\end{aligned} \tag{32}$$

where ΔT is the time step, j is the time step counter.

By substituting Eqs. (30) and (32) into the governing equations Eqs. (17)–(21) and performing some manipulations, the governing equations may be obtained as following transformed form.

$$
\begin{aligned}
&\sum_{i=0}^{L}\Bigg[\frac{\tilde{E}_1\tau_1}{1-\upsilon_1^2}(i+1)(i+3)\left(U_{i+2,j}+\frac{\tau_1}{2}X_{i+2,j}^{(1)}+\frac{\tau_2}{2}X_{i+2,j}^{(2)}\right)+\frac{\tilde{E}_3\tau_3}{1-\upsilon_3^2}(i+1)(i+3)\left(U_{i+2,j}-\frac{\tau_2}{2}X_{i+2,j}^{(2)}-\frac{\tau_3}{2}X_{i+2,j}^{(3)}\right)\\
&+\frac{\tilde{E}_1\tau_1}{1-\upsilon_1^2}\alpha_1[(i-\mu_1+1)(i-\mu_1+3)+\mu_1(i-\mu_1+2+\upsilon_1)]\left(U_{i-\mu_1+2,j}+\frac{\tau_1}{2}X_{i-\mu_1+2,j}^{(1)}+\frac{\tau_2}{2}X_{i-\mu_1+2,j}^{(2)}\right)\\
&+\frac{\tilde{E}_1\tau_1}{1-\upsilon_1^2}\beta_1[(i-\eta_1+1)(i-\eta_1+3)+\eta_1(i-\eta_1+2+\upsilon_1)]\left(U_{i-\eta_1+2,j}+\frac{\tau_1}{2}X_{i-\eta_1+2,j}^{(1)}+\frac{\tau_2}{2}X_{i-\eta_1+2,j}^{(2)}\right)\\
&+\frac{\tilde{E}_3\tau_3}{1-\upsilon_3^2}\alpha_3[(i-\mu_3+1)(i-\mu_3+3)+\mu_3(i-\mu_3+2+\upsilon_3)]\left(U_{i-\mu_3+2,j}-\frac{\tau_2}{2}X_{i-\mu_3+2,j}^{(2)}-\frac{\tau_3}{2}X_{i-\mu_3+2,j}^{(3)}\right)\\
&+\frac{\tilde{E}_3\tau_3}{1-\upsilon_3^2}\beta_3[(i-\eta_3+1)(i-\eta_3+3)+\eta_3(i-\eta_3+2+\upsilon_3)]\left(U_{i-\eta_3+2,j}-\frac{\tau_3}{2}X_{i-\eta_3+2,j}^{(3)}-\frac{\tau_2}{2}X_{i-\eta_3+2,j}^{(2)}\right)\\
&+\frac{E_2\tau_2}{1-\upsilon_2^2}(i+1)(i+3)U_{i+2,j}-\tilde{\rho}_1b^2\tau_1\left(\ddot{U}_{i,j}+\frac{\tau_1}{2}\ddot{X}_{i,j}^{(1)}+\frac{\tau_2}{2}\ddot{X}_{i,j}^{(2)}\right)-\tilde{\rho}_1b^2\tau_1\gamma_1\left(\ddot{U}_{i-\chi_1,j}+\frac{\tau_1}{2}\ddot{X}_{i-\chi_1,j}^{(1)}+\frac{\tau_2}{2}\ddot{X}_{i-\chi_1,j}^{(2)}\right)\\
&-\rho_2b^2\tau_2\ddot{U}_{i,j}-\tilde{\rho}_3b^2\tau_3\left(\ddot{U}_{i,j}-\frac{\tau_3}{2}\ddot{X}_{i,j}^{(3)}-\frac{\tau_2}{2}\ddot{X}_{i,j}^{(2)}\right)-\tilde{\rho}_3b^2\tau_3\gamma_3\left(\ddot{U}_{i-\chi_3,j}-\frac{\tau_3}{2}\ddot{X}_{i-\chi_3,j}^{(3)}-\frac{\tau_2}{2}\ddot{X}_{i-\chi_3,j}^{(2)}\right)\\
&-\tilde{\rho}_1b^2\tau_1\lambda_1\left(\ddot{U}_{i-\xi_1,j}+\frac{\tau_1}{2}\ddot{X}_{i-\xi_1,j}^{(1)}+\frac{\tau_2}{2}\ddot{X}_{i-\xi_1,j}^{(2)}\right)-\tilde{\rho}_3b^2\tau_3\lambda_3\left(\ddot{U}_{i-\xi_3,j}-\frac{\tau_3}{2}\ddot{X}_{i-\xi_3,j}^{(3)}-\frac{\tau_2}{2}\ddot{X}_{i-\xi_3,j}^{(2)}\right)\Bigg]R^i=0
\end{aligned}
\tag{33}
$$

$$
\begin{aligned}
&\sum_{i=0}^{L}\Bigg\{\frac{\tilde{E}_1\tau_1^2}{1-\upsilon_1^2}(i+1)(i+3)\left(\frac{1}{2}U_{i+2,j}+\frac{\tau_1}{3}X_{i+2,j}^{(1)}+\frac{\tau_2}{4}X_{i+2,j}^{(2)}\right)\\
&+\frac{\tilde{E}_1\tau_1^2}{1-\upsilon_1^2}\alpha_1(i-\mu_1+1)(i-\mu_1+3)\left(\frac{1}{2}U_{i-\mu_1+2,j}+\frac{\tau_1}{3}X_{i-\mu_1+2,j}^{(1)}+\frac{\tau_2}{4}X_{i-\mu_1+2,j}^{(2)}\right)\\
&+\frac{\tilde{E}_1\tau_1^2}{1-\upsilon_1^2}\beta_1(i-\eta_1+1)(i-\eta_1+3)\left(\frac{1}{2}U_{i-\eta_1+2,j}+\frac{\tau_1}{3}X_{i-\eta_1+2,j}^{(1)}+\frac{\tau_2}{4}X_{i-\eta_1+2,j}^{(2)}\right)\\
&-\frac{\tilde{E}_1\tau_1}{2(1+\upsilon_1)}\left[X_{i,j}^{(1)}+(i+1)W_{i+1,j}\right]-\frac{\tilde{E}_1\tau_1}{2(1+\upsilon_1)}\alpha_1\left[X_{i-\mu_1,j}^{(1)}+(i-\mu_1+1)W_{i-\mu_1+1,j}\right]\\
&-\frac{\tilde{E}_1\tau_1}{2(1+\upsilon_1)}\beta_1\left[X_{i-\eta_1,j}^{(1)}+(i-\eta_1+1)W_{i-\eta_1+1,j}\right]\\
&+\frac{\tilde{E}_1\tau_1^2}{2(1-\upsilon_1^2)}\alpha_1\mu_1(i-\mu_1+2+\upsilon_1)\left(U_{i-\mu_1+2,j}+\frac{\tau_1}{2}X_{i-\mu_1+2,j}^{(1)}+\frac{\tau_2}{2}X_{i-\mu_1+2,j}^{(2)}\right)\\
&+\frac{\tilde{E}_1\tau_1^2}{2(1-\upsilon_1^2)}\eta_1\beta_1(i-\eta_1+2+\upsilon_1)\left(U_{i-\eta_1+2,j}+\frac{\tau_1}{2}X_{i-\eta_1+2,j}^{(1)}+\frac{\tau_2}{2}X_{i-\eta_1+2,j}^{(2)}\right)\\
&+\frac{\tilde{E}_1\tau_1^3}{12(1-\upsilon_1^2)}\mu_1\alpha_1(i-\mu_1+2+\upsilon_1)X_{i-\mu_1+2,j}^{(1)}+\frac{\tilde{E}_1\tau_1^3}{12(1-\upsilon_1^2)}\eta_1\beta_1(i-\eta_1+2+\upsilon_1)X_{i-\eta_1+2,j}^{(1)}\\
&-\frac{b^2}{2}\tilde{\rho}_1\tau_1^2\left(\ddot{U}_{i,j}+\frac{\tau_2}{2}\ddot{X}_{i,j}^{(2)}+\frac{2\tau_1}{3}\ddot{X}_{i,j}^{(1)}\right)-\frac{b^2}{2}\tilde{\rho}_1\tau_1^2\gamma_1\left(\ddot{U}_{i-\chi_1,j}+\frac{\tau_2}{2}\ddot{X}_{i-\chi_1,j}^{(2)}+\frac{2\tau_1}{3}\ddot{X}_{i-\chi_1,j}^{(1)}\right)\\
&-\lambda_1\frac{b^2}{2}\tilde{\rho}_1\tau_1^2\left(\ddot{U}_{i-\xi_1,j}+\frac{\tau_2}{2}\ddot{X}_{i-\xi_1,j}^{(2)}+\frac{2\tau_1}{3}\ddot{X}_{i-\xi_1,j}^{(1)}\right)\Bigg\}R^i=0
\end{aligned}
\tag{34}
$$

$$
\begin{aligned}
&\sum_{i=0}^{L}\Bigg[\frac{\tilde{E}_1\tau_2\tau_1}{2(1-\upsilon_1^2)}(i+1)(i+3)\left(U_{i+2,j}+\frac{\tau_1}{2}X_{i+2,j}^{(1)}+\frac{\tau_2}{2}X_{i+2,j}^{(2)}\right)-\frac{\tilde{E}_3\tau_2\tau_3}{2(1-\upsilon_3^2)}(i+1)(i+3)\left(U_{i+2,j}-\frac{\tau_2}{2}X_{i+2,j}^{(2)}-\frac{\tau_3}{2}X_{i+2,j}^{(3)}\right)\\
&+\frac{\tilde{E}_1\tau_2\tau_1}{2(1-\upsilon_1^2)}\alpha_1[(i-\mu_1+1)(i-\mu_1+3)+\mu_1(i-\mu_1+2+\upsilon_1)]\left(U_{i-\mu_1+2,j}+\frac{\tau_1}{2}X_{i-\mu_1+2,j}^{(1)}+\frac{\tau_2}{2}X_{i-\mu_1+2,j}^{(2)}\right)\\
&+\frac{\tilde{E}_1\tau_2\tau_1}{2(1-\upsilon_1^2)}\beta_1[(i-\eta_1+1)(i-\eta_1+3)+\eta_1(i-\eta_1+2+\upsilon_1)]\left(U_{i-\eta_1+2,j}+\frac{\tau_1}{2}X_{i-\eta_1+2,j}^{(1)}+\frac{\tau_2}{2}X_{i-\eta_1+2,j}^{(2)}\right)\\
&-\frac{\tilde{E}_3\tau_2\tau_3}{2(1-\upsilon_3^2)}\alpha_3[(i-\mu_3+1)(i-\mu_3+3)-\mu_3(i-\mu_3+2+\upsilon_3)]\left(U_{i-\mu_3+2,j}-\frac{\tau_3}{2}X_{i-\mu_3+2,j}^{(3)}-\frac{\tau_2}{2}X_{i-\mu_3+2,j}^{(2)}\right)\\
&-\frac{\tilde{E}_3\tau_2\tau_3}{2(1-\upsilon_3^2)}\beta_3[(i-\eta_3+1)(i-\eta_3+3)-\eta_3(i-\eta_3+2+\upsilon_3)]\left(U_{i-\eta_3+2,j}-\frac{\tau_3}{2}X_{i-\eta_3+2,j}^{(3)}-\frac{\tau_2}{2}X_{i-\eta_3+2,j}^{(2)}\right)\\
&+\frac{E_2\tau_2^3}{12(1-\upsilon_2^2)}(i+1)(i+3)X_{i+2,j}^{(2)}-\frac{E_2\tau_2}{2(1+\upsilon_2)}\left(X_{i,j}^{(2)}+(i+1)W_{i+1,j}\right)-\frac{\tau_1\tau_2}{2}b^2\tilde{\rho}_1\left(\ddot{U}_{i,j}+\frac{\tau_1}{2}\ddot{X}_{i,j}^{(1)}+\frac{\tau_2}{2}\ddot{X}_{i,j}^{(2)}\right)\\
&-\frac{\tau_1\tau_2}{2}b^2\tilde{\rho}_1\gamma_1\left(\ddot{U}_{i-\chi_1,j}+\frac{\tau_1}{2}\ddot{X}_{i-\chi_1,j}^{(1)}+\frac{\tau_2}{2}\ddot{X}_{i-\chi_1,j}^{(2)}\right)-\frac{\tau_1\tau_2}{2}b^2\tilde{\rho}_1\lambda_1\left(\ddot{U}_{i-\xi_1,j}+\frac{\tau_1}{2}\ddot{X}_{i-\xi_1,j}^{(1)}+\frac{\tau_2}{2}\ddot{X}_{i-\xi_1,j}^{(2)}\right)\\
&+\frac{\tau_2\tau_3}{2}b^2\tilde{\rho}_3\left(\ddot{U}_{i,j}-\frac{\tau_2}{2}\ddot{X}_{i,j}^{(2)}-\frac{\tau_3}{2}\ddot{X}_{i,j}^{(3)}\right)+\frac{\tau_2\tau_3}{2}b^2\tilde{\rho}_3\gamma_3\left(\ddot{U}_{i-\chi_3,j}-\frac{\tau_2}{2}\ddot{X}_{i-\chi_3,j}^{(2)}-\frac{\tau_3}{2}\ddot{X}_{i-\chi_3,j}^{(3)}\right)\\
&+\frac{\tau_2\tau_3}{2}b^2\tilde{\rho}_3\lambda_3\left(\ddot{U}_{i-\xi_3,j}-\frac{\tau_2}{2}\ddot{X}_{i-\xi_3,j}^{(2)}-\frac{\tau_3}{2}\ddot{X}_{i-\xi_3,j}^{(3)}\right)-b^2\rho_2\frac{\tau_2^3}{12}\ddot{X}_{i,j}^{(2)}\Bigg]R^i=0
\end{aligned}
\tag{35}
$$

$$\begin{aligned}&\sum_{i=0}^{L}\Big\{-\frac{\tilde{E}_3\tau_3^2}{1-\upsilon_3^2}(i+1)(i+3)\left(\frac{1}{2}U_{i+2,j}-\frac{\tau_3}{3}X_{i+2,j}^{(3)}-\frac{\tau_2}{4}X_{i+2,j}^{(2)}\right)\\&-\frac{\tilde{E}_3\tau_3^2}{1-\upsilon_3^2}\alpha_3(i-\mu_3+1)(i-\mu_3+3)\left(\frac{1}{2}U_{i-\mu_3+2,j}+\frac{\tau_3}{3}X_{i-\mu_3+2,j}^{(3)}+\frac{\tau_2}{4}X_{i-\mu_3+2,j}^{(2)}\right)\\&-\frac{\tilde{E}_3\tau_3^2}{1-\upsilon_3^2}\beta_3(i-\eta_3+1)(i-\eta_3+3)\left(\frac{1}{2}U_{i-\eta_3+2,j}-\frac{\tau_3}{3}X_{i-\eta_3+2,j}^{(3)}-\frac{\tau_2}{4}X_{i-\eta_3+2,j}^{(2)}\right)\\&-\frac{\tilde{E}_3\tau_3}{2(1+\upsilon_3)}\left[X_{i,j}^{(3)}+(i+1)W_{i+1,j}\right]-\frac{\tilde{E}_3\tau_3}{2(1+\upsilon_3)}\alpha_3\left[X_{i-\mu_3,j}^{(3)}+(i-\mu_3+1)W_{i-\mu_3+1,j}\right]\\&-\frac{\tilde{E}_3\tau_3}{2(1+\upsilon_3)}\beta_3\left[X_{i-\eta_3,j}^{(3)}+(i-\eta_3+1)W_{i-\eta_3+1,j}\right]\\&-\frac{\tilde{E}_3\tau_3^2}{2(1-\upsilon_3^2)}\alpha_3\mu_3(i-\mu_3+2+\upsilon_3)\left(U_{i-\mu_3+2,j}-\frac{\tau_3}{2}X_{i-\mu_3+2,j}^{(3)}-\frac{\tau_2}{2}X_{i-\mu_3+2,j}^{(2)}\right)\\&-\frac{\tilde{E}_3\tau_3^2}{2(1-\upsilon_3^2)}\eta_3\beta_3(i-\eta_3+2+\upsilon_3)\left(U_{i-\eta_3+2,j}-\frac{\tau_3}{2}X_{i-\eta_3+2,j}^{(3)}-\frac{\tau_2}{2}X_{i-\eta_3+2,j}^{(2)}\right)\\&+\frac{\tilde{E}_3\tau_3^3}{12(1-\upsilon_3^2)}\mu_3\alpha_3(i-\mu_3+2+\upsilon_3)X_{i-\mu_3+2,j}^{(3)}+\frac{\tilde{E}_3\tau_3^3}{12(1-\upsilon_3^2)}\eta_3\beta_3(i-\eta_3+2+\upsilon_3)X_{i-\eta_3+2,j}^{(3)}\\&+\frac{b^2}{2}\tilde{\rho}_3\tau_3^2\left(\ddot{U}_{i,j}-\frac{\tau_2}{2}\ddot{X}_{i,j}^{(2)}-\frac{2\tau_3}{3}\ddot{X}_{i,j}^{(3)}\right)+\frac{b^2}{2}\tilde{\rho}_3\tau_3^2\gamma_3\left(\ddot{U}_{i-\chi_3,j}-\frac{\tau_2}{2}\ddot{X}_{i-\chi_3,j}^{(2)}-\frac{2\tau_3}{3}\ddot{X}_{i-\chi_3,j}^{(3)}\right)\\&+\lambda_3\frac{b^2}{2}\tilde{\rho}_3\tau_3^2\left(\ddot{U}_{i-\xi_3,j}-\frac{\tau_2}{2}\ddot{X}_{i-\xi_3,j}^{(2)}-\frac{2\tau_3}{3}\ddot{X}_{i-\xi_3,j}^{(3)}\right)\Big\}R^i=0\end{aligned}\tag{36}$$

$$\begin{aligned}&\sum_{i=0}^{L}\Big\{\left[\frac{\tilde{E}_1\tau_1}{2(1+\upsilon_1)}+\frac{E_2\tau_2}{2(1+\upsilon_2)}+\frac{\tilde{E}_3\tau_3}{2(1+\upsilon_3)}\right](i+2)^2W_{i+2,j}+\frac{\tilde{E}_1\tau_1}{2(1+\upsilon_1)}\alpha_1(i-\mu_1+2)^2W_{i-\mu_1+2,j}\\&\frac{\tilde{E}_1\tau_1}{2(1+\upsilon_1)}\beta_1(i-\eta_1+2)^2W_{i-\eta_1+2,j}+\frac{\tilde{E}_3\tau_3}{2(1+\upsilon_3)}\alpha_3(i-\mu_3+2)^2W_{i-\mu_3+2,j}\\&+\frac{\tilde{E}_3\tau_3}{2(1+\upsilon_3)}\beta_3(i-\eta_3+2)^2W_{i-\eta_3+2,j}+\frac{\tilde{E}_1\tau_1}{2(1+\upsilon_1)}(i+2)X_{i+1,j}^{(1)}+\frac{\tilde{E}_1\tau_1}{2(1+\upsilon_1)}\alpha_1(i-\mu_1+2)X_{i-\mu_1+1,j}^{(1)}\\&+\frac{\tilde{E}_1\tau_1}{2(1+\upsilon_1)}\beta_1(i-\eta_1+2)X_{i-\eta_1+1,j}^{(1)}+\frac{E_2\tau_2}{2(1+\upsilon_2)}(i+2)X_{i+1,j}^{(2)}+\frac{\tilde{E}_3\tau_3}{2(1+\upsilon_3)}(i+2)X_{i+1,j}^{(3)}\\&+\frac{\tilde{E}_3\tau_3}{2(1+\upsilon_3)}\alpha_3(i-\mu_3+2)X_{i-\mu_3+1,j}^{(3)}+\frac{\tilde{E}_3\tau_3}{2(1+\upsilon_3)}\beta_3(i-\eta_3+2)X_{i-\eta_3+1,j}^{(3)}\\&+\frac{\tilde{E}_1\tau_1}{2(1+\upsilon_1)}\mu_1\alpha_1\left(X_{i-\mu_1+1,j}^{(1)}+(i-\mu_1+2)W_{i-\mu_1+2,j}\right)+\frac{\tilde{E}_1\tau_1}{2(1+\upsilon_1)}\eta_1\beta_1\left(X_{i-\eta_1+1,j}^{(1)}+(i-\eta_1+2)W_{i-\eta_1+2,j}\right)\\&+\frac{\tilde{E}_3\tau_3}{2(1+\upsilon_3)}\mu_3\alpha_3\left(X_{i-\mu_3+1,j}^{(3)}+(i-\mu_3+2)W_{i-\mu_3+2,j}\right)+\frac{\tilde{E}_3\tau_3}{2(1+\upsilon_3)}\eta_3\beta_3\left(X_{i-\eta_3+1,j}^{(3)}+(i-\eta_3+2)W_{i-\eta_3+2,j}\right)\\&+q(t=j\Delta t)\delta(i)-b^2(\tilde{\rho}_1\tau_1+\rho_2\tau_2+\tilde{\rho}_3h_3)\ddot{W}_{i,j}-b^2\tilde{\rho}_1\tau_1\gamma_1\ddot{W}_{i-\chi_1,j}-b^2\tilde{\rho}_1\tau_1\lambda_1\ddot{W}_{i-\xi_1,j}-b^2\tilde{\rho}_3h_3\gamma_3\ddot{W}_{i,-\chi_3 j}\\&-b^2\tilde{\rho}_3h_3\lambda_3\ddot{W}_{i-\xi_3,j}\Big\}R^i=0\end{aligned}\tag{37}$$

By substituting Eqs. (30) and (31) into the boundary conditions Eqs. (22)–(26), the transformed forms of the boundary conditions become:

$$\begin{aligned}&\sum_{i=0}^{L}\Big[\frac{\tilde{E}_1\tau_1}{1-\upsilon_1^2}(1+\alpha_1+\beta_1)(i+\upsilon_1)\left(U_{i,j}+\frac{\tau_1}{2}X_{i,j}^{(1)}+\frac{\tau_2}{2}X_{i,j}^{(2)}\right)+\frac{E_2\tau_2}{1-\upsilon_2^2}(i+\upsilon_2)U_{i,j}\\&\frac{\tilde{E}_3\tau_3}{1-\upsilon_3^2}(1+\alpha_3+\beta_3)(\upsilon)\left(U_{i,j}-\frac{\tau_3}{2}X_{i,j}^{(3)}-\frac{\tau_2}{2}X_{i,j}^{(2)}\right)+(\tau_1+\tau_2+\tau_3)b\left(k_uU_{i,j}+C_u\dot{U}_{i,j}\right)+\\&\frac{\tau_1^2}{2}b\left(k_uX_{i,j}^{(1)}+C_u\dot{X}_{i,j}^{(1)}\right)+\frac{\tau_2}{2}(\tau_1-\tau_3)b\left(k_uX_{i,j}^{(2)}+C_u\dot{X}_{i,j}^{(2)}\right)-\frac{\tau_3^2}{2}b\left(k_uX_{i,j}^{(3)}+C_u\dot{X}_{i,j}^{(3)}\right)\Big]=0\end{aligned}\tag{38}$$

$$\begin{aligned}&\sum_{i=0}^{L}\Big[\frac{\tilde{E}_1\tau_1^2}{2(1-\upsilon_1^2)}(i+\upsilon_1)\left(U_{i,j}+\frac{\tau_1}{2}X_{i,j}^{(1)}+\frac{\tau_2}{2}X_{i,j}^{(2)}\right)(1+\alpha_1+\beta_1)+\frac{\tilde{E}_1\tau_1^3}{12(1-\upsilon_1^2)}(i+\upsilon_1)X_{i,j}^{(1)}(1+\alpha_1+\beta_1)+\\&\frac{\tau_1^3}{12}b\left(k_uX_{i,j}^{(1)}+C_u\dot{X}_{i,j}^{(1)}\right)+\frac{\tau_1^2}{2}bk_u\left(U_{i,j}+\frac{\tau_1}{2}X_{i,j}^{(1)}+\frac{\tau_2}{2}X_{i,j}^{(2)}\right)+\frac{\tau_1^2}{2}bC_u\left(\dot{U}_{i,j}+\frac{\tau_1}{2}\dot{X}_{i,j}^{(1)}+\frac{\tau_2}{2}\dot{X}_{i,j}^{(2)}\right)\Big]=0\end{aligned}\tag{39}$$

$$\sum_{i=0}^{L}\left[\frac{\tilde{E}_1\tau_1\tau_2}{2(1-\upsilon_1^2)}(i+\upsilon_1)\left(U_{i,j}+\frac{\tau_1}{2}X_{i,j}^{(1)}+\frac{\tau_2}{2}X_{i,j}^{(2)}\right)(1+\alpha_1+\beta_1)+\frac{E_2\tau_2^3}{12(1-\upsilon_2^2)}(i+\upsilon_2)X_{i,j}^{(2)}\right.$$
$$-\frac{\tilde{E}_3\tau_2\tau_3}{2(1-\upsilon_3^2)}(1+\alpha_3+\beta_3)(i+\upsilon_3)\left(U_{i,j}-\frac{\tau_3}{2}X_{i,j}^{(3)}-\frac{\tau_2}{2}X_{i,j}^{(2)}\right)+\frac{\tau_2}{2}(\tau_1-\tau_3)b(k_uU_{i,j}+C_u\dot{U}_{i,j}) \tag{40}$$
$$\left.+\frac{\tau_2\tau_1^2}{4}b\left(k_uX_{i,j}^{(1)}+C_u\dot{X}_{i,j}^{(1)}\right)+\frac{\tau_2^2}{4}\left(\tau_1+\frac{\tau_2}{3}+\tau_3\right)b\left(k_uX_{i,j}^{(2)}+C_u\dot{X}_{i,j}^{(2)}\right)+\frac{\tau_2\tau_3^2}{4}b\left(k_uX_{i,j}^{(3)}+C_u\dot{X}_{i,j}^{(3)}\right)\right]=0$$

$$\sum_{i=0}^{L}\left[-\frac{\tilde{E}_3\tau_3^2}{2(1-\upsilon_3^2)}(1+\alpha_3+\beta_3)(i+\upsilon_3)\left(U_{i,j}-\frac{\tau_3}{2}X_{i,j}^{(3)}-\frac{\tau_2}{2}X_{i,j}^{(2)}\right)+\frac{\tilde{E}_3\tau_3^3}{12(1-\upsilon_3^2)}(i+\upsilon_3)X_{i,j}^{(3)}(1+\alpha_3+\beta_3)+\right.$$
$$\left.\frac{\tau_3^3}{12}b\left(k_uX_{i,j}^{(3)}+C_u\dot{X}_{i,j}^{(3)}\right)-\frac{\tau_3^2}{2}bk_u\left(U_{i,j}-\frac{\tau_3}{2}X_{i,j}^{(3)}-\frac{\tau_2}{2}X_{i,j}^{(2)}\right)-\frac{\tau_3^2}{2}bC_u\left(\dot{U}_{i,j}-\frac{\tau_3}{2}\dot{X}_{i,j}^{(3)}-\frac{\tau_2}{2}\dot{X}_{i,j}^{(2)}\right)\right]=0 \tag{41}$$

$$\sum_{i=0}^{L}\left[\frac{\tilde{E}_1\tau_1}{2(1+\upsilon_1)}\left(X_{i,j}^{(1)}+iW_{i,j}\right)(1+\alpha_1+\beta_1)+\frac{E_2\tau_2}{2(1+\upsilon_2)}\left(X_{i,j}^{(2)}+iW_{i,j}\right)+\frac{\tilde{E}_3\tau_3}{2(1+\upsilon_3)}\left(X_{i,j}^{(3)}+iW_{i,j}\right)(1+\alpha_3+\beta_3)\right.$$
$$\left.+k_wW_{i,j}+C_w\dot{W}_{i,j}\right]=0 \tag{42}$$

Based on the Eq. (30), the regularity conditions Eq. (27) at the center of the axisymmetric plate $R=0$ may be satisfied as:

$$\begin{aligned}
&u|_{R=0}=0\Rightarrow\sum_{i=0}^{L}U_{i,j}R^i\Big|_{R=0}=0\Rightarrow U_{0,j}=0,\\
&\psi_r^{(1)}\Big|_{R=0}=0\Rightarrow\sum_{x=0}^{X}X_{i,j}^{(1)}R^i\Big|_{R=0}=0\Rightarrow X_{0,j}^{(1)}=0,\\
&\psi_r^{(2)}\Big|_{R=0}=0\Rightarrow\sum_{x=0}^{X}X_{i,j}^{(2)}R^i\Big|_{R=0}=0\Rightarrow X_{0,j}^{(2)}=0,\\
&\psi_r^{(3)}\Big|_{R=0}=0\Rightarrow\sum_{x=0}^{X}X_{i,j}^{(3)}R^i\Big|_{R=0}=0\Rightarrow X_{0,j}^{(3)}=0,\\
&w|_{R=0}=0\Rightarrow\sum_{x=0}^{X}W_{i,j}R^i\Big|_{R=0}=0\Rightarrow W_{0,j}=0.
\end{aligned} \tag{43}$$

The initial conditions can be obtained as following transformed forms:

$$U_{i,0}=\dot{U}_{i,0}=0,\quad X_{i,0}^{(1)}=\dot{X}_{i,0}^{(1)}=0,\quad X_{i,0}^{(2)}=\dot{X}_{i,0}^{(2)}=0,\quad X_{i,0}^{(3)}=\dot{X}_{i,0}^{(3)}=0,\quad W_{i,0}=\dot{W}_{i,0}=0, \tag{44}$$

Based on the fourth-order Runge–Kutta numerical time integration method, the acceleration and velocity parameters at $t=(j+1)\Delta t$ can be found by using the following formulations [52]:

$$\ddot{Y}(R,t=(j+1)\Delta t)=\frac{4}{\Delta t^2}\left[Y(R,t=(j+1)\Delta t)-Y(R,t=j\Delta t)-\Delta t\dot{Y}(R,t=j\Delta t)-\frac{1}{4}\Delta t^2\ddot{Y}(R,t=j\Delta t)\right] \tag{45}$$

$$\dot{Y}(R,t=(j+1)\Delta t)=\dot{Y}(R,t=j\Delta t)+\frac{\Delta t}{2}[\ddot{Y}(R,t=j\Delta t)-\ddot{Y}(R,t=(j+1)\Delta t)] \tag{46}$$

The transformed form of Eqs. (44) and (45) may be expressed as:

$$\ddot{Y}_{i,j+1}=\frac{4}{\Delta t^2}\left(Y_{i,j+1}-Y_{i,j}-\Delta t\dot{Y}_{i,j}-\frac{1}{4}\Delta t^2\ddot{Y}_{i,j}\right) \tag{47}$$

$$\dot{Y}_{i,j+1}=\dot{Y}_{i,j}+\frac{\Delta t}{2}(\ddot{Y}_{i,j}-\ddot{Y}_{i,j+1}) \tag{48}$$

In solving the resulting system of equations, the transformed forms of the governing equations Eqs. (33)–(37), edge conditions Eqs. (38)–(42), regularity conditions Eq. (43), initial conditions Eq. (44) and fourth-order Runge–Kutta equations Eq. (46) and (47) have to be used.

Initial values of the acceleration parameters $\ddot{U}_{i,0}$, $\ddot{X}_{i,0}^{(1)}$, $\ddot{X}_{i,0}^{(2)}$, $\ddot{X}_{i,0}^{(3)}$ and $\ddot{W}_{i,0}$ are obtained by substituting the initial conditions into the governing equations for $j=0$. By substituting Eq. (47) into the governing equations Eqs. (33)–(37), substituting Eq. (48) into the edge conditions Eqs. (38)–(42) and using the regularity conditions Eq. (43), unknown parameters at the end of each time step will be determined. This procedure must be repeated till the final time instant is reached.

4. Results and discussions

In the present section, effects of the in-plane and transverse stiffness and damping coefficients of the viscoelastic edge supports on the transient response of the sandwich plates are investigated. In this regard, various examples of sandwich plates subjected to various dynamic loads are introduced.

Forced dynamic analysis of sandwich plates with vicoelastic/elastic boundary supports have not been carried out yet, so results of sandwich plates with the classical edge conditions (ideal clamped and simply supported edge) as some special cases of the vicoelastic/elastic supports are compared with those extracted from the ABAQUS software based on the 3D theory of elasticity.

Results of the three-dimensional theory of elasticity are extracted from ABAQUS by using quadratic eight-node axisymmetric elements (CAX8R) with radial and transverse nodal displacements. Also time step 10^{-5} (s) is used in the implicit dynamic numerical time integration procedure.

In order to investigate the dynamic response of sandwich circular structures with viscoelastic boundary support, a three-layered asymmetric annular sandwich plate with the following material properties and thickness ratios is considered:

$$\begin{array}{lllll} \text{Top facesheet}: & \tilde{E}_1 = 68\,\text{GPa}, & \tilde{\rho}_1 = 1840\,\text{kg/m}^3, & \upsilon_1 = 0.3, & \tau_1 = 0.1 \\ \text{Core}: & E_2 = 70\,\text{GPa}, & \rho_2 = 1200\,\text{kg/m}^3, & \upsilon_2 = 0.25, & \tau_2 = 0.2 \\ \text{Bottom facesheet}: & \tilde{E}_3 = 110\,\text{GPa}, & \tilde{\rho}_3 = 2350\,\text{kg/m}^3, & \upsilon_3 = 0.25, & \tau_3 = 0.1 \end{array}$$

In the presented results, following inhomogeneity parameters are used for heterogeneous face sheets:

$$\begin{array}{llll} \alpha_1 = \gamma_1 = 0.4, & \beta_1 = \lambda_1 = 0.2, & \mu_1 = \chi_1 = 1, & \eta_1 = \xi_1 = 2 \\ \alpha_3 = \gamma_3 = \beta_3 = \lambda_3 = 0.3, & \mu_3 = \chi_3 = 1, & \eta_3 = \xi_3 = 2 & \end{array}$$

Based on the mentioned parameters, material properties of the heterogeneous face sheets will be as follow:

$$\begin{array}{ll} E_1(r) = 68[1+0.4R+0.2R^2]\,\text{GPa}, & \rho_1(r) = 1840[1+0.4R+0.2R^2]\,\text{kg/m}^3 \\ E_3(r) = 110[1+0.3(R+R^2)]\,\text{GPa}, & \rho_3(r) = 2350[1+0.3(R+R^2)]\,\text{kg/m}^3 \end{array}$$

Also, the sandwich plate with homogeneous face sheets can be analyzed when α_1, β_1, α_3, β_3, γ_1, λ_1, γ_3 and λ_1 are set to zero, and material properties of homogeneous face sheets will be:

$$\begin{array}{ll} E_1 = \tilde{E}_1 = 68\,\text{GPa}, & \rho_1 = \tilde{\rho}_1 = 1840\,\text{kg/m}^3 \\ E_3 = \tilde{E}_3 = 110\,\text{GPa}, & \rho_3 = \tilde{\rho}_3 = 2350\,\text{kg/m}^3 \end{array}$$

In this study, sandwich plates under various dynamic loads $F = PT(t)$ are examined, in which P is the maximum intensity and $T(t)$ is a unit function in time domain. Dynamic response analyses of the sandwich circular plates are performed for maximum intensity of $P = 1$ MPa and the following unit functions in time domain:

- Step function: $T(t) = H(t)$.
- Pulse function for a time duration t_0: $T(t) = H(t) - H(t - t_0)$.
- Sinusoidal function: $T(t) = \sin(\omega t)$.
- Trapezoidal function for a period $4Tp$ (as shown in Fig. 2):

$$T(t) = \begin{cases} \dfrac{t-4(i-1)T_p}{T_p} & \text{for } 4(i-1)T_p \le t \le (4i-3)T_p \\ 1 & \text{for } (4i-3)T_p \le t \le (4i-2)T_p \\ 1-\dfrac{t-(4i-2)T_p}{T_p} & \text{for } (4i-2)T_p \le t \le (4i-1)T_p \\ 0 & \text{for } (4i-1)T_p \le t \le 4iT_p \end{cases} \quad i = 1, 2, 3, \ldots$$

where $H(t)$ is Heaviside's step function.

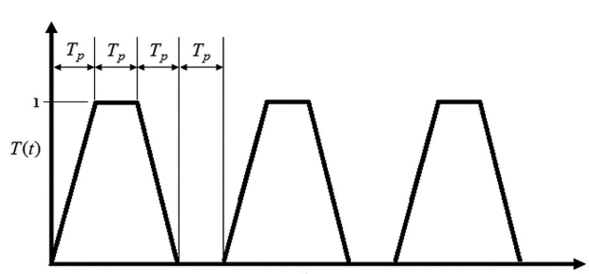

Fig. 2 – Loading with trapezoidal time history.

In this section, transient response of sandwich plate under viscoelastic edge supports are examined for various values of in-plane and transverse stiffness k_u, k_w (N/m^2) and damping C_u, C_w (N/m^2 s) coefficients. Since the maximum deflection of the axisymmetric circular plate occurs at the center of the plate, results of the dynamic response are presented for $R = 0$.

4.1. Transient response of sandwich plates with classical boundary conditions

The accuracy and efficiency of the obtained results based on the proposed semi-analytical solution are verified in this example. In the case of ideal classical boundary conditions (simply supported and clamped edge), dynamic response of homogeneous and heterogeneous sandwich plates which obtained based on the layerwise theory (LW) are compared with results of the three-dimensional theory of elasticity (3D) which extracted from ABAQUS finite element software.

The ideal classical boundary conditions may be simulated by setting the stiffness and damping parameters of viscoelastic edges as follows:

- Ideal clamped edge: $C_u = C_w = 0,\ k_u, k_w \to \infty\ (k_u = k_w = 10^{40})$.
- Ideal simply supported edge: $C_u = C_w = k_u = 0,\ k_w \to \infty\ (k_w = 10^{40})$.

The time variations of the central deflection of the homogenous sandwich plate under the trapezoidal periodic loading are presented in Fig. 3. Loading with trapezoidal time history is an intermediate case between the harmonic and step loading. It is worth to be mentioned that the trapezoidal periodic loading in contrast the ideal rectangular loading is a feasible loading for experimental test. On the other hand, this case of loading includes ramps and constant parts, which are two important load cases for dynamic analysis of structures. As Fig. 3 shows, the global dynamic behavior of plate has a trapezoidal shaped pattern with local oscillations.

For better investigation of the differences between results of central deflections obtained by LW method and results of finite element software (ABAQUS), the presented results in Fig. 3(b) are analyzed in Table 1. It may be noted that there is good agreement between the results.

The time variations of the central deflection of the heterogeneous plate under the sinusoidal loading are shown in Fig. 4 for various excitation frequencies. As it may be readily seen, period of harmonic loadings have not a significant effect on the amplitude of vibration. Also, the period of the lateral deflection is same as the period of loading.

The comparisons reveal that there is a good agreement between present results and results of ABAQUS software, even

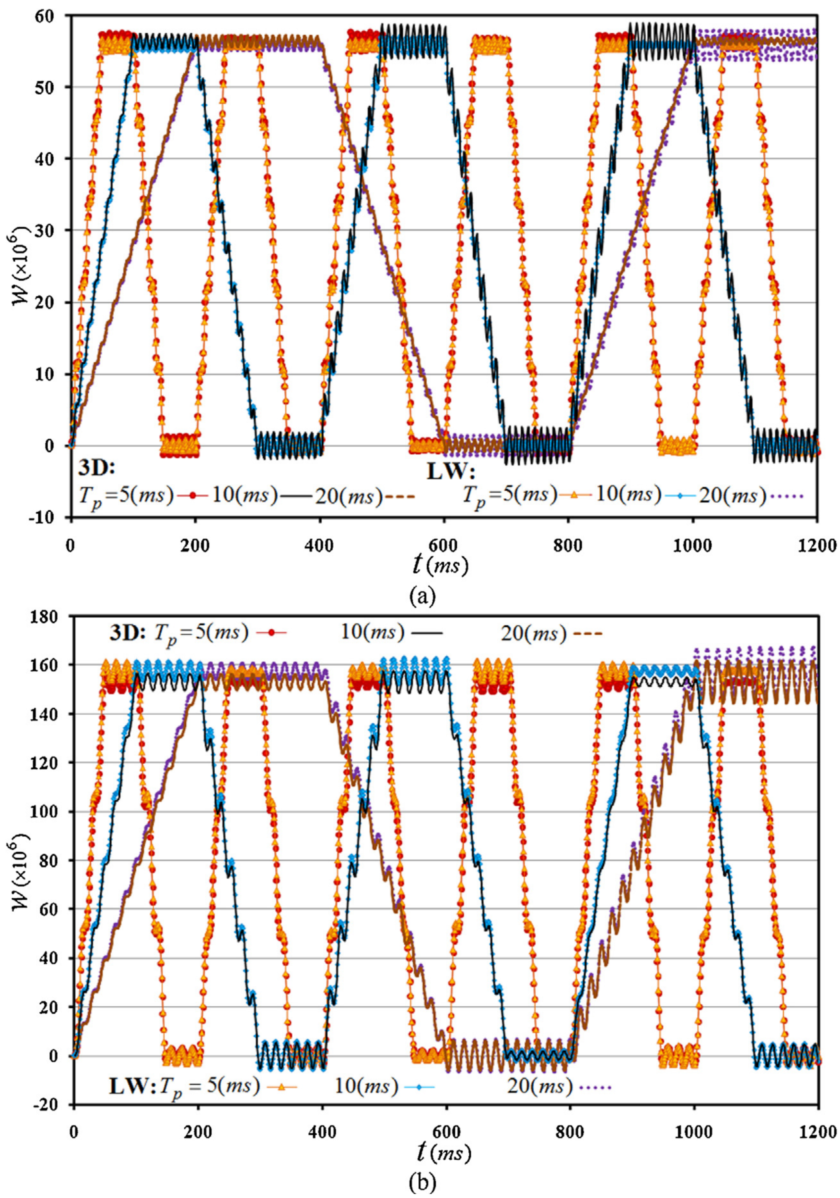

Fig. 3 – The central deflection of the homogenous sandwich plate under the trapezoidal periodic loading: (a) clamped and (b) simply supported boundary conditions.

Table 1 – Comparison between central deflections obtained by LW method and results of finite element software (ABAQUS) for homogenous sandwich plate with simply supported edge under the trapezoidal periodic loading.

t (ms)	T_p = 5 ms			T_p = 10 ms			T_p = 20 ms		
	3D (ABAQUS)	LW	Difference (%)	3D (ABAQUS)	LW	Difference (%)	3D (ABAQUS)	LW	Difference (%)
10	0.0802	0.0792	1.27	0.0401	0.0396	1.27	0.0198	0.0198	0.13
100	156.16	160.72	2.92	156.41	161.02	2.94	78.308	80.633	2.97
200	−2.886	−2.934	−1.64	151.44	155.82	2.89	152.75	157.25	2.95
300	150.24	154.57	2.88	0.7731	0.7709	0.28	156.04	160.7	2.99
400	−2.749	−2.725	−0.88	−2.902	−3.0079	−3.66	149.92	154.19	2.85
500	154.75	159.36	2.98	155.83	160.52	3.01	72.002	73.935	2.68
600	−1.26	−1.222	−3.05	156.01	161	3.2	−5.858	−6.1954	−5.8
700	156.37	161.16	3.06	−0.678	−0.669	−1.29	3.9697	4.3715	10.1
800	8.374	8.6984	3.87	5.0188	5.5326	10.2	−1.745	−1.7476	−0.2
900	154.63	159.07	2.87	154.54	158.63	2.65	83.303	85.958	3.19
1000	3.898	3.9725	1.91	153.01	157.23	2.76	161.54	166.96	3.36

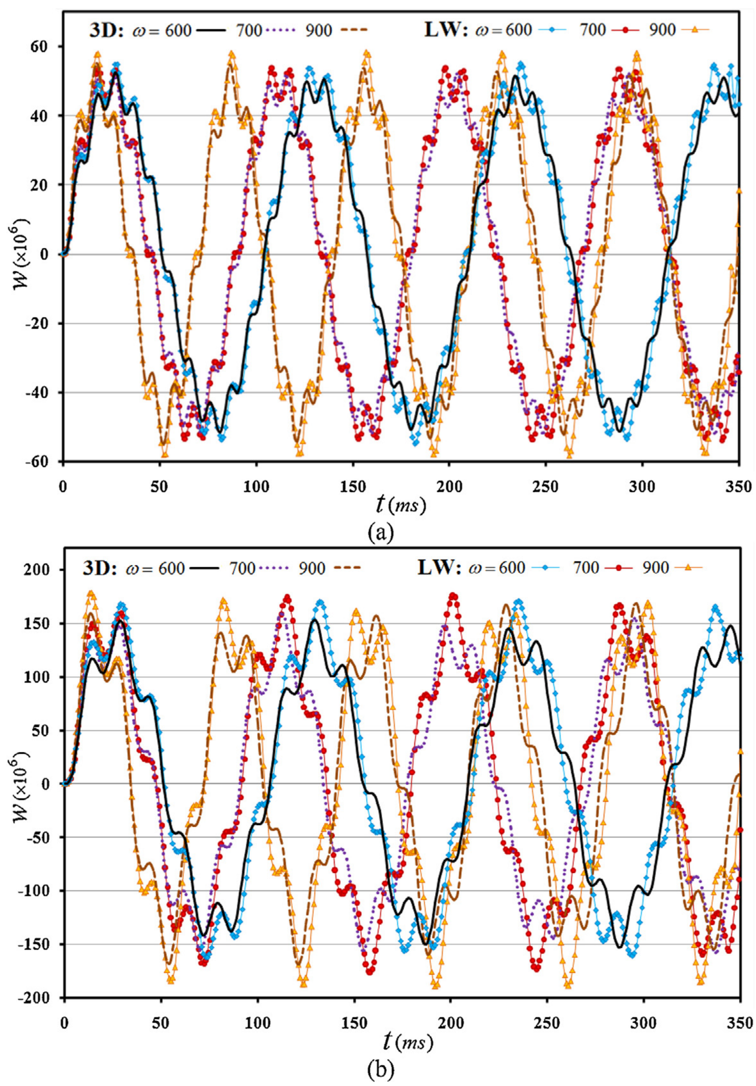

Fig. 4 – The central deflection of the heterogeneous sandwich plate under the sinusoidal loading: (a) clamped and (b) simply supported boundary conditions.

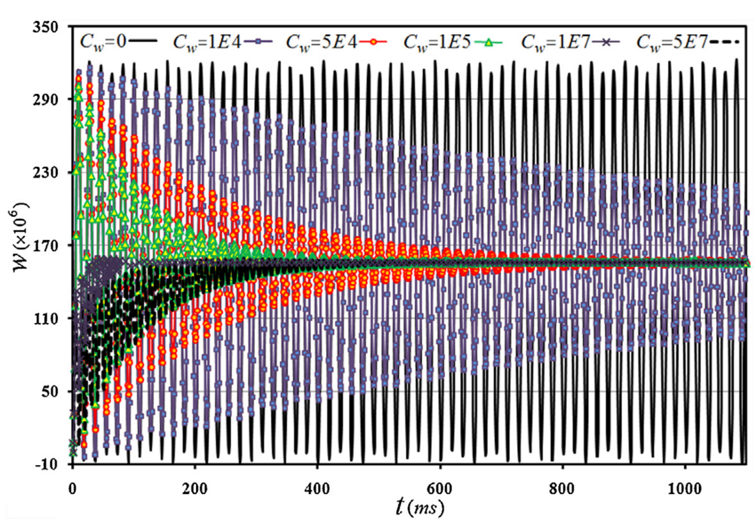

Fig. 5 – The effects of the transverse damping coefficients of the viscoelastic edge supports on the dynamic behavior of homogeneous sandwich plate under the step loading.

for thick sandwich plates with heterogeneous face sheets and asymmetric lay-ups.

4.2. The effects of the transverse stiffness and damping coefficients of the viscoelastic edge supports

To evaluate the effects of the transverse stiffness and damping coefficients of the viscoelastic edge supports (C_w and k_w) on the dynamic behavior of sandwich plate, results of the present research are presented for $C_u = 0$, $k_u = 0$ and $k_u \to \infty$.

The time variations of the central deflection of the plate under step loading are presented in Fig. 5 for $k_w = 5E9$, $k_u \to \infty$ and various transverse damping coefficients of the viscoelastic edge supports ($C_w = 0$, 1E4, 4E4, 1E5, 1E7 and 5E7). This figure shows that when there is no damping in the edge supports ($C_w = 0$), the plate oscillates about the static deflection (deflection of plate based on the static analysis for $C_w = 0$) with constant amplitude. The vibration amplitude of plate with viscoelastic edge supports decreases with time and tends to the static response, due to the dissipation of system energy. As expected, the vibration amplitude of plate decreases as the damping coefficient of supports increases. This figure also shows that for plate with transverse damping coefficients of $C_w = 1E7$ and 5E7, as time goes on, the maximum deflection increases in each cycle and approaches the final position (static response). In the other words, the lateral deflection does not exceed the static deflection. It is interesting to note that the plate with $C_w = 1E7$ approaches the final position in a shorter time than the other mentioned cases, even in comparison with the plate with the higher transverse damping coefficient $C_w = 5E7$.

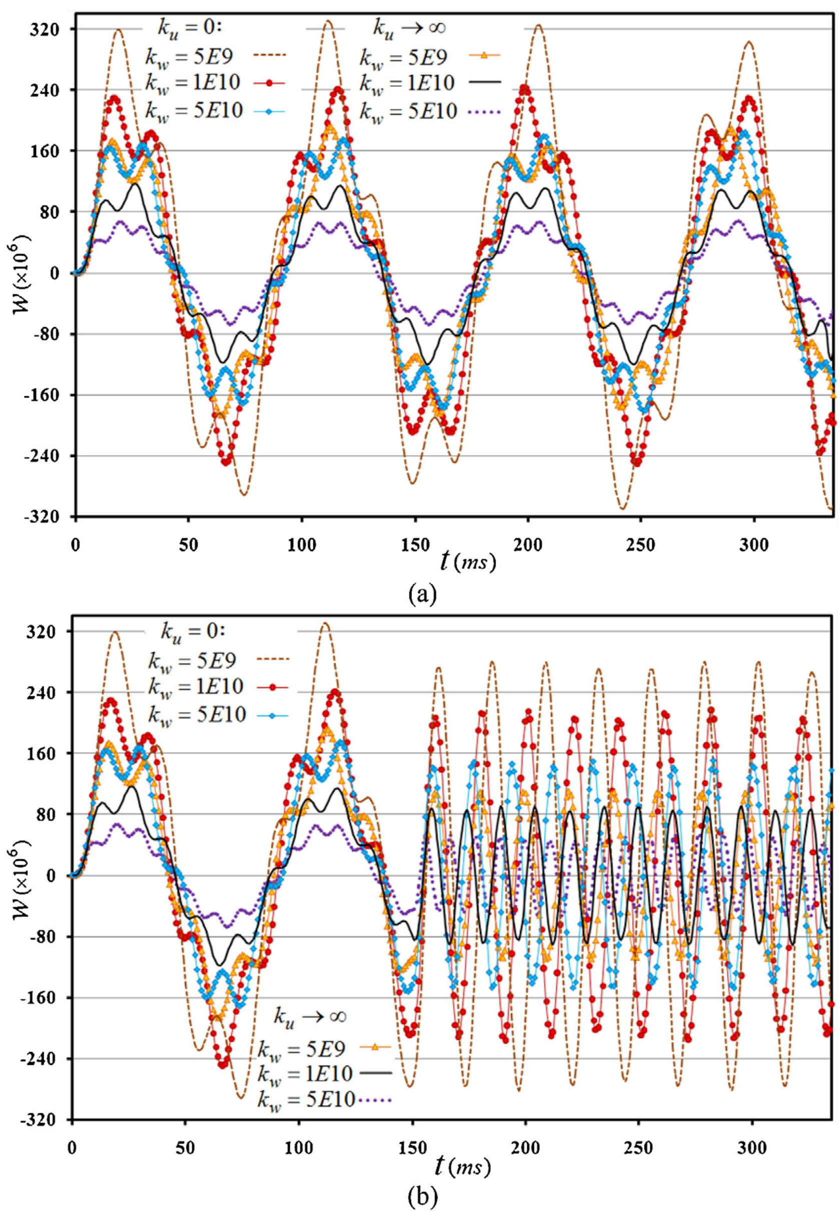

Fig. 6 – The effects of the transverse and in-plane stiffness coefficients of the viscoelastic edge supports on the dynamic behavior of heterogeneous sandwich plate under (a) the sinusoidal loading and (b) the pulse loading.

The effects of the transverse stiffness coefficients of the edge supports on the dynamic behavior of sandwich plate subjected to the sinusoidal and pulse loadings are illustrated in Fig. 6(a) and (b), respectively, in which $C_w = C_u = 0$. It is observed that with increasing the transverse stiffness coefficients, rigidity of B.Cs decreases the vibration amplitude and increases the natural vibration frequency of plate (vibration frequency of plate subjected to the pulse loading when the load is removed).

The effects of the transverse viscoelastic edge supports on the dynamic behavior of sandwich plate under the sinusoidal loading is depicted in Fig. 7. It can be seen that the dynamic response of plates with viscoelastic edge supports is smoother and the local oscillations are eliminated.

The effects of the transverse damping coefficients of viscoelastic edge supports on the dynamic behavior of sandwich plate under the sinusoidal pulse loadings are depicted in Figs. 8 and 9 for $k_u = 0$ and $k_u \to \infty$, respectively. Figs. 8(a) and 9(a) show that by increasing damping value up to 1E6, the vibration amplitude will be decreased and damped out more rapidly. It is interesting to note that the vibration amplitude of plate with $C_w = 1E6$ is damped out more rapidly than plate with $C_w = 1E7$. Also it can be seen from Figs. 8(b) and 9(b) that by increasing damping value from 1E7 to ∞(1E40), the vibration amplitude will be increased when the load is removed. For $C_w \to \infty(1E40)$ dynamic response of plate tend to behavior of simply supported (Fig. 8(b)) and clamped (Fig. 9 (b)) plates without energy dissipation. The mentioned dynamic responses are also expected based on the related boundary condition (Eq. (26)), this equation can be rewritten for $C_w \to \infty(1E40)$ as $(C_w \dot{w})_{r=b} = 0 \to \dot{w} = 0 \to w = 0$.

Indeed, energy dissipation of plate (elimination or reduction of the oscillations) is depend on two parameters; damping coefficient and velocity of edge. By increasing the damping

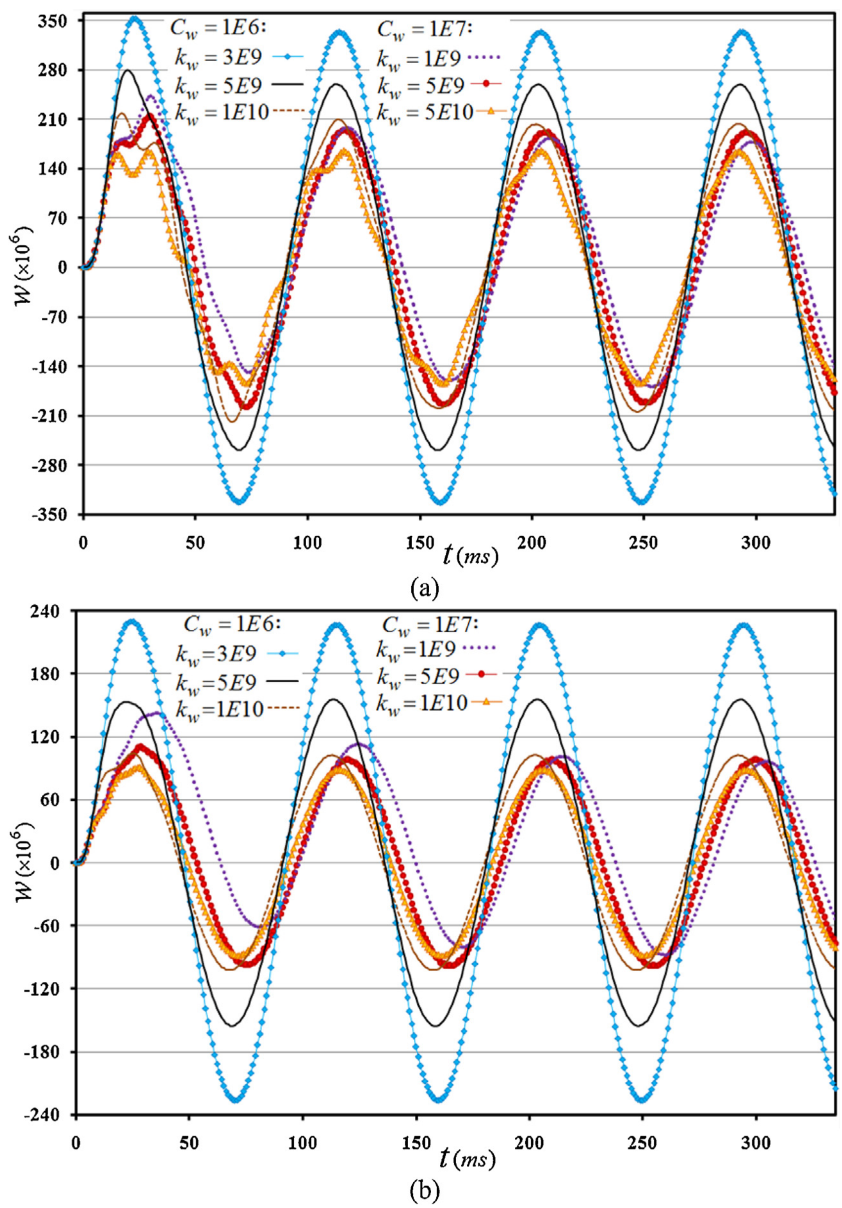

Fig. 7 – The effects of the transverse stiffness and damping coefficients of the viscoelastic edge supports on the dynamic behavior of heterogeneous sandwich plate under the sinusoidal loading ($f(t) = \sin(700t)$) for $C_u = 0$: (a) $k_u = 0$ and (b) $k_u \to \infty$.

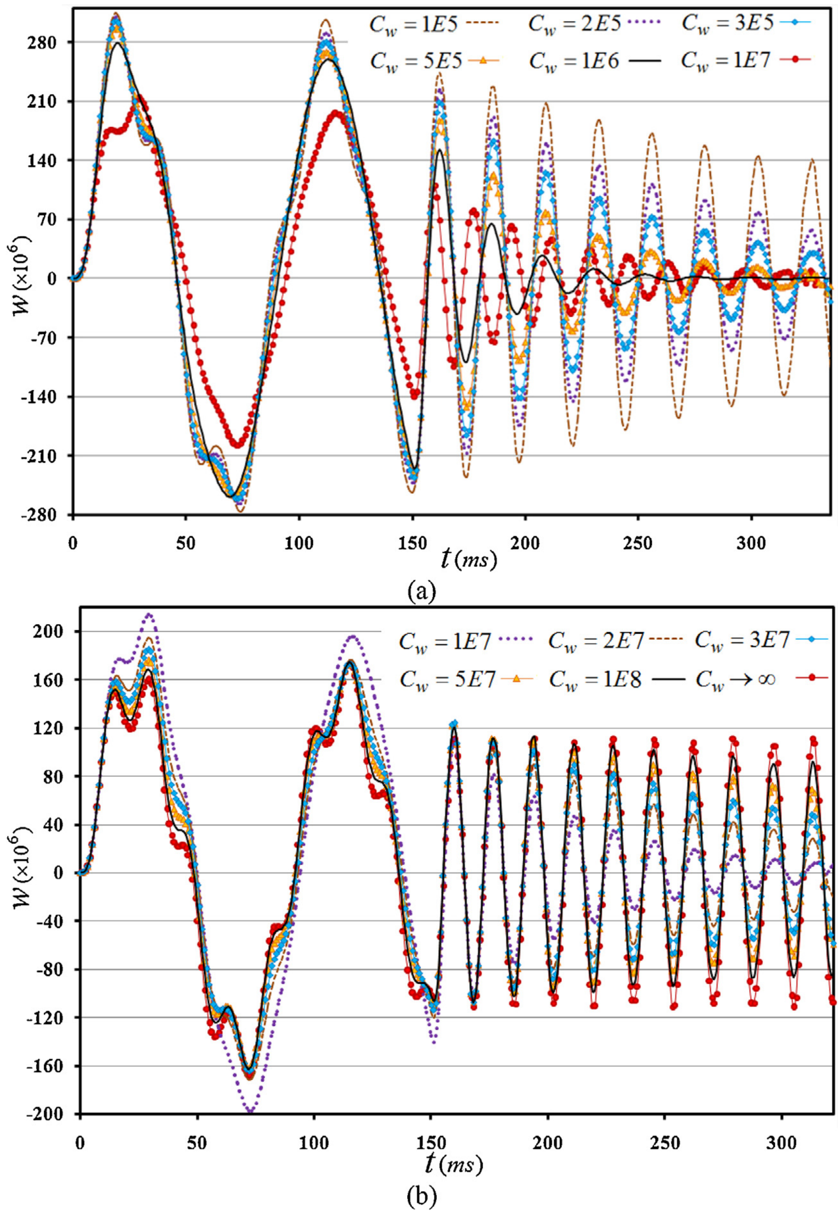

Fig. 8 – The effects of the transverse damping coefficients of the viscoelastic edge supports on the dynamic behavior of heterogeneous sandwich plate under pulse loading for $k_w = 5E9$, $C_u = 0$ and $k_u = 0$.

coefficient, rigidity of the edge supports will be increased, therefore velocity of the edge will be reduced.

The obtained results reveal that there is an optimum damping coefficient for elimination or reduction of the oscillations.

4.3. The effects of the in-plane stiffness and damping coefficients of the viscoelastic edge supports

In this example, a sensitivity analysis is performed to show the effects of the in-plane stiffness and damping coefficients of the viscoelastic edge supports on the transient response of sandwich plate. In this regard, the central deflections of the heterogeneous sandwich plate with elastically restrained edge subjected to the pulse loading are presented in Fig. 10, when the boundary condition tends from the simply supported to the clamped edge ($C_u = C_w = 0$, $k_w \to \infty$). Four different values of in-plane stiffness coefficients, $K_u = 0$ (ideal simply supported edge), $k_u \to \infty$ (ideal clamped edge), K_u = 1E11 and 5E11 (in the range between simply supported and clamped edges) are considered.

Also in the case of the ideal classical boundary conditions, dynamic responses of the sandwich plates with heterogeneous face sheets which obtained based on the layerwise theory (LW) are compared with those of finite element method based on the three-dimensional theory of elasticity (3D). In the present relatively complicated case (dynamic response of asymmetric sandwich plate with heterogeneous face sheets), a

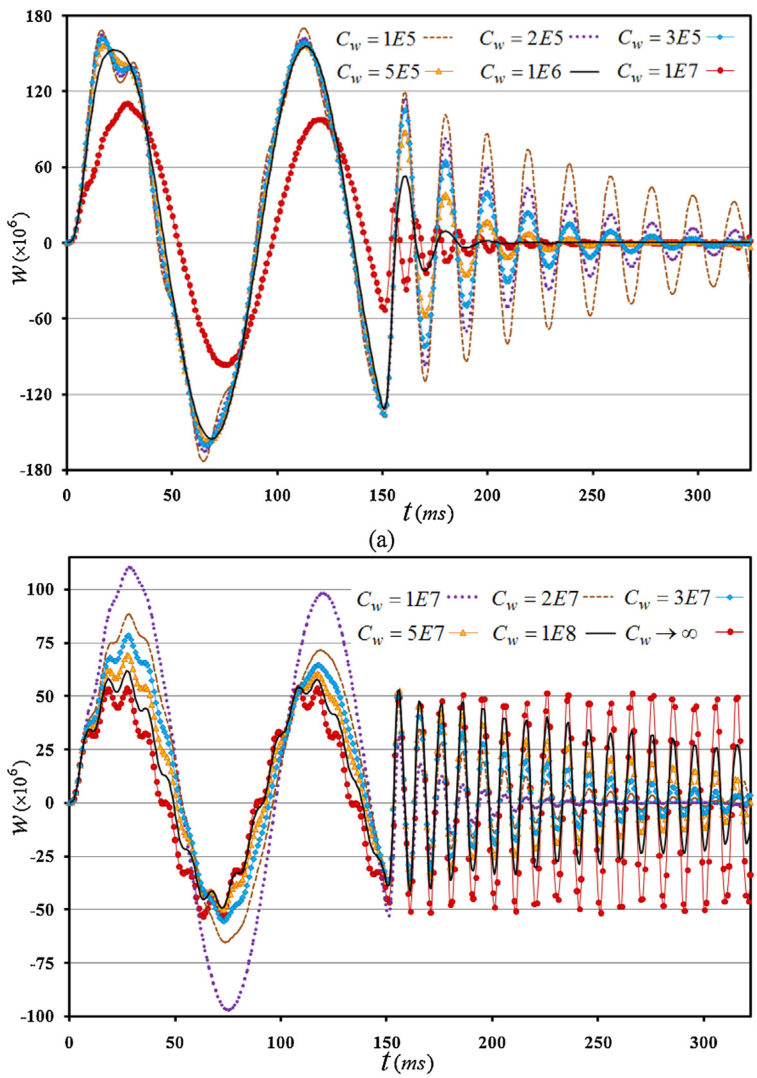

Fig. 9 – The effects of the transverse damping coefficients of the viscoelastic edge supports on the dynamic behavior of heterogeneous sandwich plate under pulse loading for $k_w = 5E9$, $C_u = 0$ and $k_u \to \infty$.

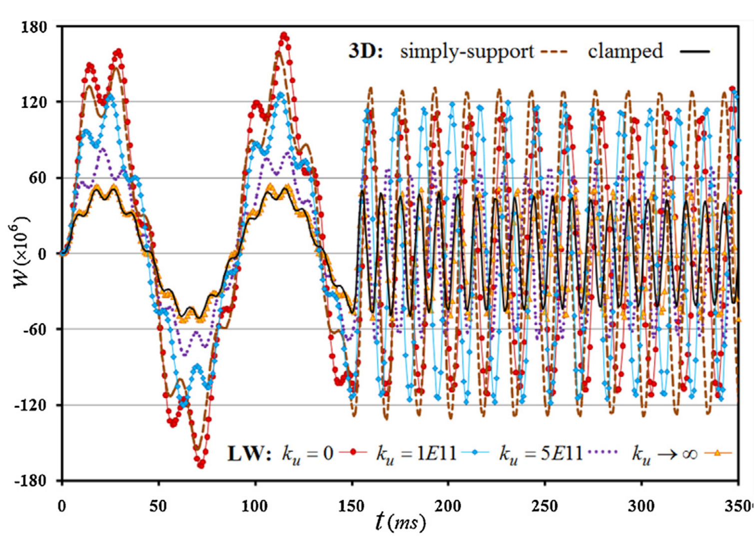

Fig. 10 – The central deflection of the heterogeneous sandwich plate under the pulse loading.

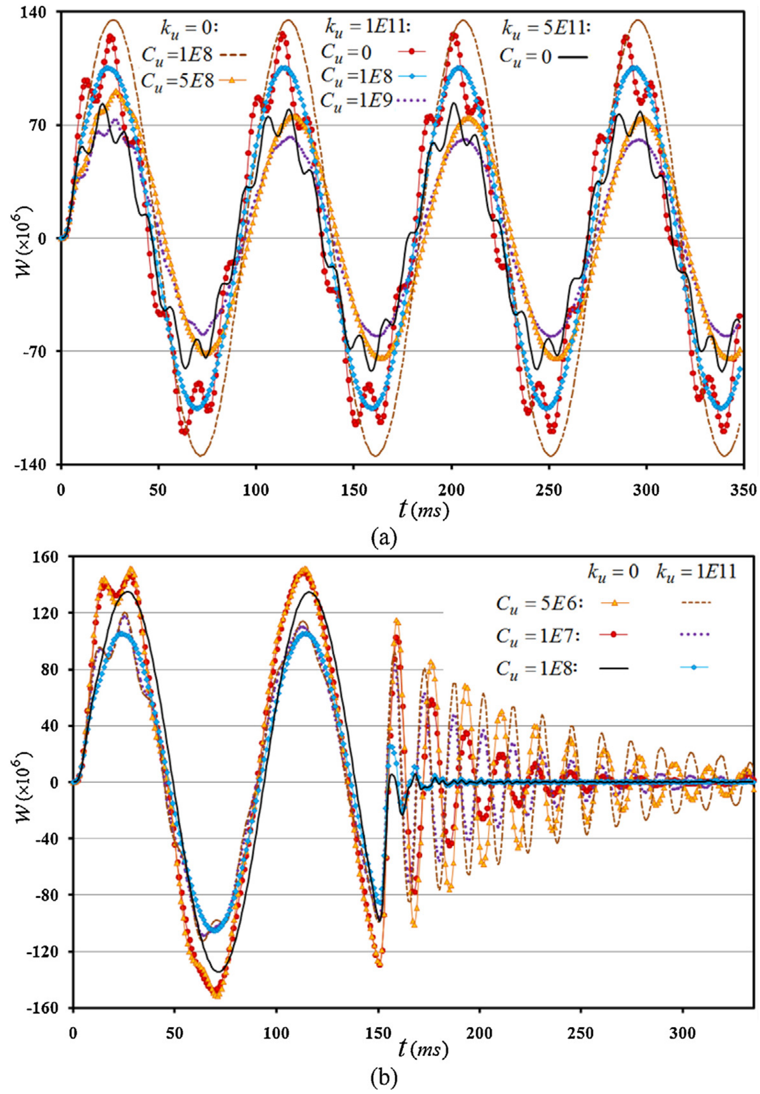

Fig. 11 – The effects of the in-plane stiffness and damping coefficients of the viscoelastic edge supports on the dynamic behavior of heterogeneous sandwich plate under (a) the sinusoidal loading and (b) the pulse loading.

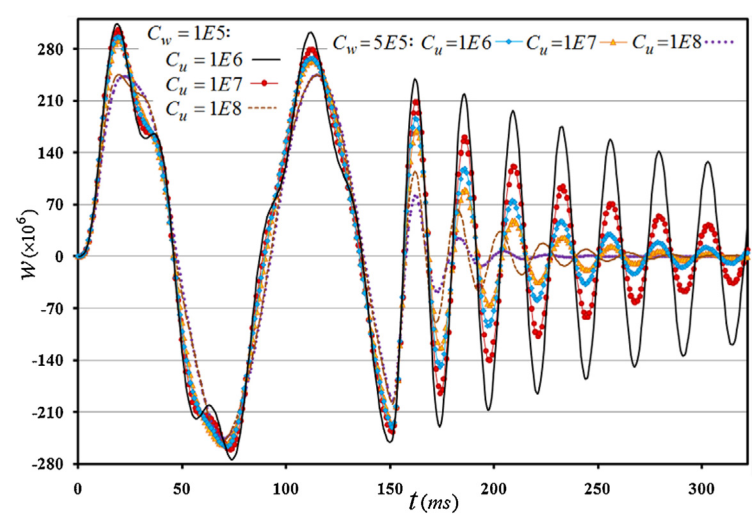

Fig. 12 – The effects of the transverse and in-plane damping coefficients of the viscoelastic edge supports on the dynamic behavior of heterogeneous sandwich plate under the pulse loading.

good agreement exists between results of the present theory and results of the three-dimensional theory of elasticity. As expected and the figure also shows, when the boundary condition tends from the simply supported to the clamped edge, the amplitude decreases and the natural frequency increases.

The effects of the in-plane stiffness and damping coefficients of the edge supports on the dynamic behavior of sandwich plate subjected to the sinusoidal and the pulse loadings are illustrated in Fig. 11(a) and (b) for $k_w \to \infty$, respectively.

The effects of the in-plane and transverse damping coefficients of the edge supports on the dynamic behavior of sandwich plate subjected to the pulse loading are simultaneously shown in Fig. 12 for $K_w = 5E9$, $K_u = 1E8$ and a series of damping coefficients $C_w = 1E5$, $5E5$ and $C_u = 1E6$, $1E7$, $1E8$. As it may be readily seen, using viscoelastic boundary supports have led to completely smooth time variations of the lateral deflection.

5. Conclusions

In the present study, transient response of sandwich circular plate with viscoelastic boundary support is investigated for the first time. The boundary condition is simulated as viscoelastic support by using in-plane parallel translational springs and dashpots along the in-plane and transverse directions. Based on the assumed variations for the material properties of the face sheets, the proposed solution procedure may be used for a wide range of the sandwich plates with heterogeneous face sheets. To achieve more accurately results, the governing differential equations of motion are derived based on the layerwise theory. A semi-analytical method based on the power series solution and the fourth-order Runge–Kutta procedure is developed for analysis of these structures. A comprehensive sensitivity analysis is presented for evaluation of the viscoelastic edge supports effects on the transient response of sandwich plate. Results reveal that the sandwich circular plates with heterogeneous face sheets under various dynamic loads and viscoelastic boundary support may be analyzed by using the proposed solution procedure.

REFERENCES

[1] H.S. Shen, J. Yang, L. Zhang, Dynamic response of Reissner–Mindlin plates under thermomechanical loading and resting on elastic foundation, Journal of Sound and Vibration 232 (2) (2000) 309–329.

[2] O. Civalek, Nonlinear analysis of thin rectangular plates on Winkler–Pasternak elastic foundations by DSC–HDQ methods, Applied Mathematical Modelling 31 (2007) 606–624.

[3] P. Ribeiro, Non-linear forced vibrations of thin/thick beams and plates by the finite element and shooting methods, Computers & Structures 82 (2004) 1413–1423.

[4] P. Ribeiro, Forced periodic vibrations of laminated composite plates by a p-version, first order shear deformation, finite element, Composites Science and Technology 66 (2006) 1844–1856.

[5] W.L.A. Pereira, V.J. Karam, J.A.M. Carrer, W.J. Mansur, A dynamic formulation for the analysis of thick elastic plates by the boundary element method, Engineering Analysis with Boundary Elements 36 (2012) 1138–1150.

[6] H.M. Sedighi, F. Daneshmand, J. Zare, The influence of dispersion forces on the dynamic pull-in behavior of vibrating nano-cantilever based NEMS including fringing field effect, Archives of Civil and Mechanical Engineering 14 (2014) 766–775.

[7] B. Khalfi, A. Ross, Transient and harmonic response of a sandwich with partial constrained layer damping: a parametric study, Composites Part B: Engineering 91 (2016) 44–55.

[8] L. Sator, V. Sladek, J. Sladek, L. Young Sator, V. Sladek, J. Sladek, D.L. Young, Elastodynamics of FGM plates by mesh-free method, Composite Structures 140 (2016) 309–322.

[9] Z.X. Wanga, H.S. Shen, Nonlinear dynamic response of sandwich plates with FGM face sheets resting on elastic foundations in thermal environments, Ocean Engineering 57 (2013) 99–110.

[10] A.R. Mojdehi, A. Darvizeh, A. Basti, H. Rajabi, Three dimensional static and dynamic analysis of thick functionally graded plates by the meshless local Petrov–Galerkin (MLPG) method, Engineering Analysis with Boundary Elements 35 (2011) 1168–1180.

[11] M.M. Alipour, M. Shariyat, Semi-analytical consistent zigzag-elasticity formulations with implicit layerwise shear correction factors for dynamic stress analysis of sandwich circular plates with FGM layers, Composites Part B: Engineering 49 (2013) 43–64.

[12] M.M. Alipour, M. Shariyat, Analytical zigzag-elasticity transient and forced dynamic stress and displacement response prediction of the annular FGM sandwich plates, Composite Structures 106 (2013) 426–445.

[13] T. Kocatürk, G. Altintas, Determination of the steady-state response of viscoelastically point-supported rectangular orthotropic plates, Mechanics of Composite Materials 39 (5) (2003) 455–466.

[14] T. Kocatürk, S. Sezer, C. Demir, The effect of support locations on the steady-state response of viscoelastically point-supported rectangular orthotropic plates, Archive of Applied Mechanics 75 (2005) 58–67.

[15] M. Stembalski, W. Skoczyński, A. Roszkowski, P. Preś, Testing the vibration damping of a glass gatherer robot arm using a friction damper, Archives of Civil and Mechanical Engineering 17 (2017) 240–248.

[16] F. Alinaghizadeh, M. Shariati, Geometrically non-linear bending analysis of thick two-directional functionally graded annular sector and rectangular plates with variable thickness resting on non-linear elastic foundation, Composites Part B 86 (2016) 61–83.

[17] F. Alinaghizadeh, M. Shariati, Buckling analysis of variable thickness radially functionally graded annular sector plates resting on two-parameter elastic foundations by the GDQ method, International Journal of Applied Mechanics 7 (2015) 1550083.

[18] Sh. Hosseini-Hashemi, H. Rokni Damavandi Taher, H. Akhavan, Vibration analysis of radially FGM sectorial plates of variable thickness on elastic foundations, Composite Structures 92 (2010) 1734–1743.

[19] Sh. Hosseini-Hashemi, H. Akhavan, H. Rokni Damavandi Taher, N. Daemi, A. Alibeigloo, Differential quadrature analysis of functionally graded circular and annular sector plates on elastic foundation, Materials and Design 31 (2010) 1871–1880.

[20] A. Nosier, F. Fallah, Non-linear analysis of functionally graded circular plates under asymmetric transverse loading, International Journal of Non-Linear Mechanics 44 (2009) 928–942.

[21] S.Y. Lee, S.M. Lin, Levy-type solution for the analysis of nonuniform plates, Computers & Structures 49 (6) (1993) 931–939.

[22] L.G. Nallim, B.M. Luccioni, R.O. Grossi, Vibration of general triangular composite plates with elastically restrained edges, Thin-Walled Structures 43 (2005) 1711–1745.
[23] L.G. Nallim, R.O. Grossi, Vibration of angle-ply symmetric laminated composite plates with edges elastically restrained, Composite Structures 81 (2007) 80–83.
[24] L.G. Nallim, R.O. Grossi, Natural frequencies of symmetrically laminated elliptical and circular plates, International Journal of Mechanical Sciences 50 (2008) 1153–1167.
[25] R. Vescovini, C. Bisagni, Single-mode solution for post-buckling analysis of composite panels with elastic restraints loaded in compression, Composites Part B: Engineering 43 (2012) 1258–1274.
[26] E. Bahmyari, A. Rahbar-Ranji, Free vibration analysis of orthotropic plates with variable thickness resting on non-uniform elastic foundation by element free Galerkin method, Journal of Mechanical Science and Technology 26 (9) (2012) 2685–2694.
[27] A.S. Ashour, Vibration of angle-ply symmetric laminated composite plates with edges elastically restrained, Composite Structures 74 (2006) 294–302.
[28] L.B. Rao, C.K. Rao, Fundamental buckling of circular plates with elastically restrained edges and resting on concentric rigid ring support, Frontiers of Mechanical Engineering 8 (3) (2013) 291–297.
[29] L.B. Rao, C.K. Rao, Buckling of circular plate with foundation and elastic edge, International Journal of Mechanical and Materials Engineering 11 (2015) 149–156.
[30] L.B. Rao, C.K. Rao, Frequencies of circular plate with concentric ring and elastic edge support, Frontiers of Mechanical Engineering 9 (2) (2014) 168–176.
[31] L.B. Rao, C.K. Rao, Frequency analysis of annular plates with inner and outer edges elastically restrained and resting on Winkler foundation, International Journal of Mechanical Sciences 81 (2014) 184–194.
[32] Q. Chen, P. Qiao, Post-buckling behavior of imperfect laminated composite plates with rotationally-restrained edges, Composite Structures 125 (2015) 117–126.
[33] G. Jin, H. Chen, J. Du, T. Yang, W. Li, The influence of edge restraining stiffness on the transverse vibrations of rectangular plate structures, Journal of Marine Science and Application 9 (2010) 393–402.
[34] P. Malekzadeh, M.R. Golbahar Haghighi, M.M. Atashi, Free vibration analysis of elastically supported functionally graded annular plates subjected to thermal environment, Meccanica 46 (2011) 893–913.
[35] A. Sharma, Free vibration of moderately thick antisymmetric laminated annular sector plates with elastic edge constraints, International Journal of Mechanical Sciences 83 (2014) 124–132.
[36] P.C. Dumir, C.H.R. Kumar, M.L. Gandhi, Nonlinear axisymmetric vibration of orthotropic thin circular plates with elastically restrained edges, Computers & Structures 22 (4) (1986) 677–686.
[37] M.L. Gandhi, P.C. Dumir, Y. Nath, Nonlinear axisymmetric static analysis of orthotropic thin circular plates with elastically restrained edge, Computers & Structures 20 (5) (1985) 841–853.
[38] Q. Wang, D. Shi, Q. Liang, X. Shi, A unified solution for vibration analysis of functionally graded circular, annular and sector plates with general boundary conditions, Composites Part B: Engineering 88 (2016) 264–294.
[39] T. Ye, G. Jin, Z. Su, Y. Chen, A modified Fourier solution for vibration analysis of moderately thick laminated plates with general boundary restraints and internal line supports, International Journal of Mechanical Sciences 80 (2014) 29–46.
[40] Y. Zhang, J. Du, T. Yang, Z. Liu, A series solution for the in-plane vibration analysis of orthotropic rectangular plates with elastically restrained edges, International Journal of Mechanical Sciences 79 (2014) 15–24.
[41] D. Shi, Q. Wang, X. Shi, F. Pang, A series solution for the in-plane vibration analysis of orthotropic rectangular plates with non-uniform elastic boundary constraints and internal line supports, Archive of Applied Mechanics 85 (2015) 51–73.
[42] F.A. Fazzolaria, E. Carrera, Free vibration analysis of sandwich plates with anisotropic face sheets in thermal environment by using the hierarchical trigonometric Ritz formulation, Composites Part B: Engineering 50 (2013) 67–81.
[43] E. Carrera, S. Brischetto, A survey with numerical assessment of classical and refined theories for the analysis of sandwich plates, Applied Mechanics Reviews 62 (1) (2008) 010803–010819.
[44] E. Carrera, On the use of the Murakami's zig-zag function in the modeling of layered plates and shells, Computers and Structures 82 (2004) 541–554.
[45] M.M. Alipour, A novel economical analytical method for bending and stress analysis of functionally graded sandwich circular plates with general elastic edge conditions, subjected to various loads, Composites Part B: Engineering 95 (2016) 48–63.
[46] M.M. Alipour, Effects of elastically restrained edges on FG sandwich annular plates by using a novel solution procedure based on layerwise formulation, Archives of Civil and Mechanical Engineering 16 (2016) 678–694.
[47] M.M. Alipour, M. Shariyat, An analytical global-local Taylor transformation-based vibration solution for annular FGM sandwich plates supported by nonuniform elastic foundations, Archives of Civil and Mechanical Engineering 14 (2014) 6–24.
[48] M.M. Alipour, An analytical approach for bending and stress analysis of cross/angle-ply laminated composite plates under arbitrary non-uniform loads and elastic foundations, Archives of Civil and Mechanical Engineering 16 (2) (2016) 193–210.
[49] M.M. Alipour, M. Shariyat, Analytical zigzag formulation with 3D elasticity corrections for bending and stress analysis of circular/annular composite sandwich plates with auxetic cores, Composite Structures 132 (2015) 175–197.
[50] M.M. Alipour, M. Shariyat, Analytical layerwise free vibration analysis of circular/annular composite sandwich plates with auxetic cores, International Journal of Mechanical and Materials Engineering 13 (2017) 125–157.
[51] M. Shariyat, M.M. Alipour, Analytical bending and stress analysis of variable thickness FGM auxetic conical/cylindrical shells with general tractions, Latin American Journal of Solids and Structures 14 (2017) 805–843.
[52] J. Reddy, An Introduction to the Finite Element Method, 2nd ed., Wiley, New York, 2006.
[53] A.J.M. Ferreira, Analysis of composite plates using a layerwise theory and multiquadrics discretization, Mechanics of Advanced Materials and Structures 12 (2005) 99–112.
[54] B. Liu, A.J.M. Ferreira, Y.F. Xing, A.M.A. Neves, Analysis of functionally graded sandwich and laminated shells using a layerwise theory and a differential quadrature finite element method, Composite Structures 136 (2016) 546–553.